

AN ANALYSIS OF THE EFFECT OF HELIUM ON THE  
PERFORMANCE OF A CESIATED THERMIONIC DIODE

by

Reay Stewart Dick, Jr.

---

A Thesis Submitted to the Faculty of the  
DEPARTMENT OF NUCLEAR ENGINEERING  
In Partial Fulfillment of the Requirements  
For the Degree of  
MASTER OF SCIENCE  
In the Graduate College  
THE UNIVERSITY OF ARIZONA

1 9 7 2

STATEMENT BY AUTHOR

This thesis has been submitted in partial fulfillment of requirements for an advanced degree at The University of Arizona and is deposited in the University Library to be made available to borrowers under rules of the Library.

Brief quotations from this thesis are allowable without special permission, provided that accurate acknowledgment of source is made. Requests for permission for extended quotation from or reproduction of this manuscript in whole or in part may be granted by the head of the major department or the Dean of the Graduate College when in his judgment the proposed use of the material is in the interests of scholarship. In all other instances, however, permission must be obtained from the author.

SIGNED: Ray Stewart Dick

APPROVAL BY THESIS DIRECTOR

This thesis has been approved on the date shown below:

M. V. Davis

M. V. Davis

Professor of Nuclear Engineering

8 Sept 71  
Date

## ACKNOWLEDGMENTS

The author wishes to offer his deepest thanks and gratitude to Dr. Monte V. Davis, without whose help and guidance this thesis would never have been completed.

An extra-special thanks goes to Marian Slavin for seeing this through to completion, and to Ned Britt who was of enormous aid in the formulation of this thesis.

Thanks go to the Nuclear Engineering Department at The University of Arizona for their unfailing assistance during the writing of this thesis and to Argonne National Laboratory and the library staff there, for their assistance.

## TABLE OF CONTENTS

	Page
LIST OF ILLUSTRATIONS . . . . .	v
LIST OF TABLES . . . . .	vii
ABSTRACT . . . . .	viii
1. INTRODUCTION . . . . .	1
2. DIODE OPERATING CHARACTERISTICS . . . . .	8
Ion Balance . . . . .	12
Electron Transport . . . . .	14
3. ELECTRON DIFFUSION CHANGES . . . . .	20
Evaluation . . . . .	23
Ion Current . . . . .	23
Electron Current . . . . .	24
4. ENERGY TRANSPORT . . . . .	35
Cesium Energy Transport . . . . .	35
Radiative Energy Transport . . . . .	37
Electron Energy Transport . . . . .	38
Inert Gas Energy Transfer . . . . .	43
5. CONCLUSIONS AND RESULTS . . . . .	48
APPENDIX A: DIFFUSION OF ELECTRONS THROUGH THE PLASMA . . . . .	53
APPENDIX B: ENERGY TRANSPORT FROM THE INTERELECTRODE SPACE . . . . .	55
APPENDIX C: ENERGY BALANCE ON THE EMITTER . . . . .	58
REFERENCES . . . . .	62

## LIST OF ILLUSTRATIONS

Figure	Page
1. The Effect of Inert Gas Overpressure on Diode Output . . . .	6
2. Diode Output as Short Circuit Current versus Argon Overpressure . . . . .	7
3. IV Trace for Ideal and Normal Operation, after Razor . . . .	9
4. Electron Motive Diagram Corresponding to the Transition Point . . . . .	11
5. Variation of Plasma Potential with Position . . . . .	15
6. Dependence of Arc Maintenance Drop $V_d$ upon Transition Current Density $J$ , on Emitter Temperature and the Pressure-Spacing Product . . . . .	16
7. Dependence of Electron Temperature $T_{eE}$ at Emitter Edge of Plasma on Pressure-Spacing Product $pd$ in the Ignited Mode . .	17
8. Work Function of Surface Refluxed with Cesium Vapor . . . . .	18
9. Electron Density versus Position . . . . .	25
10. Collision Probability $(\text{cm-mmHg})^{-1}$ versus Electron Energy $(\sqrt{\text{volts}})$ . . . . .	26
11. Normalized Electron Density versus Inert Gas Overpressure . .	28
12. Normalized Temperature versus Inert Gas Pressure (torr) . . .	29
13. Cesium Cross-Section . . . . .	30
14. Normalized Cross-Section versus Inert Gas Pressure (torr) . .	31
15. Normalized Velocity versus Inert Gas Pressure . . . . .	33
16. Normalized Diode Current versus Inert Gas Pressure . . . . .	34
17. Gas Conductivity $(\text{watts}/^\circ\text{K-cm}^2)$ versus Cesium Reservoir Temperature $(^\circ\text{K})$ . . . . .	36

LIST OF ILLUSTRATIONS--Continued

Figure	Page
18. Radiative Net Heat Transfer versus Hot Surface Temperature for Several Materials . . . . .	39
19. Emitter Electron Cooling Changes . . . . .	40
20. The Change in Power Output with Gas Pressure Due to Current Reflection . . . . .	42
21. Thermal Conductivities $\lambda$ of Helium and Argon as a Function of Pressure. $\lambda^\infty$ Observed Thermal Conductivity at Atmospheric Pressure . . . . .	45
22. Thermal Conductivities $\lambda$ of Helium and Argon as a Function of Pressure for a 2 mil gap, where $p^* \equiv 1$ torr and $\lambda^\infty \equiv$ Conductivity at Atmospheric Pressure . . . . .	46
23. Inert Gas Heat Transfer (watts/cm <sup>2</sup> ) versus Inert Gas Pressure (torr) for a Gap of 2 mils and $\Delta T = 1000^\circ K$ . . . . .	47
24. Summary of the Effects of Inert Gas Introduction on a Cesium Thermionic Diode with a 2 mil Spacing and $T_{cs} = 645^\circ K$ . . . . .	50
25. Normalized Diode Output versus Inert Gas Overpressure for a 2 mil Spacing . . . . .	51
26. Normalized Diode Output versus Inert Gas Overpressure for a 10 mil Spacing, with Experimental Data Plotted for Argon Only . . . . .	52
B-1 Power Loss from Interelectrode Gap Due to Gas Transport at Various Spacings, Assuming a One Inch Diameter Planar Electrode Diode . . . . .	57

LIST OF TABLES

Table	Page
1. Fission Products that May Escape from the Fuel . . . . .	3
2. Results of Kaplan Experiments . . . . .	4

## ABSTRACT

The effects of introducing helium or argon into the interelectrode space of a cesiated thermionic diode was analyzed with respect to changes in the electron transport in the plasma and changes in energy transport between the electrodes.

The operational parameters of the diode were determined in a manner consistent with a model taken from the literature.

Using those parameters the relative effects of inert gas heat transfer, cesium gas heat transfer, thermal radiation, and electron energy transport. The electron transport changes were analyzed using the Boltzmann equation, with input data taken from the literature.

The results are given for the 0-8 torr pressure range of helium and argon, and predict for close spaced diodes (<5 mil) that the heat transfer by the inert gases will be the dominant mechanism causing the reduction in diode electrical output power.

## CHAPTER 1

### INTRODUCTION

Direct energy conversion processes have, over the past fifteen years come into wider and wider use as small, low efficiency, space power plants, and as reliable solid state power units. This need has fathered many advances in thermionics, thermoelectrics, fuel cells, and other conversion devices.

Thermionic conversion has received no small amount of attention due to its promised and reliability.

Basically, a thermionic energy converter consists of two electrodes in a vacuum,<sup>1,2,3</sup> one electrode (the emitter) is heated, and the other electrode (the collector) is cooled. Electrons, thermionically emitted from the emitter flow to the collector. Connecting the two via an external load completes the circuit. One of the most important advantages of thermionic energy conversion is the high temperature rejection of heat. This is of great advantage in space power systems, which rely upon radiative cooling, or in a topping cycle on a more conventional power system.

This high temperature operating condition (1500-2000°K) of the thermionic conversion system has encountered many materials problems. The refractory metals appear to be the most suited for the system. These include Ta, Mo, W, Re, Ir, Nb, and various alloys of these metals.

Whether the system conceived for heating the emitter is a nuclear reactor or a radioactive isotope the problem of the pressure build-up of gaseous by-products is considered serious. For example consider swelling, or the effect of these gases on the operation of the diode should the gases escape to the interelectrode space.

Although in an isotope system the only gaseous product considered would be helium, the nuclear reactor system would produce a number of gaseous products, the most prolific of which are shown in Table 1.

Due to the small interelectrode spacings ( $<.01$  in) necessary to achieve reasonable output powers from the diode, the swelling of the emitter due to gas pressure is a major consideration. One solution to this problem is venting the fuel to allow the gas to escape.

The possibility of the intrusion of these gases into the interelectrode space requires a knowledge of what effect these gases have on diode output.

The effects of several inert gases on the output power of an operating diode have been studied in recent years, and the conclusions reached often are contradictory.

The results of an early experiment<sup>4</sup> reported that the power output increased with increased xenon pressure. The results of one report is recorded in Table 2. The same paper also reported a drop in output upon the addition of neon gas in the interelectrode space.

The explanation for this behavior most probably lies in the fact that very small quantities of oxygen can change the work function

Table 1. Fission Products that May Escape from the Fuel\*

Element	% Yield	Vapor Pressure
Xenon	21.8	Gas @ 300°C
Cesium	19.2	1 torr @ 300°C
Strontium	9.3	$10^{-6}$ torr @ 300°C
Barium	3.7	$10^{-8}$ torr @ 300°C
Krypton	3.9	Gas @ 300°C
Rubidium	3.5	0.6 torr @ 300°C
Tellurium	2.4	$10^{-4}$ torr @ 300°C
Iodine	0.9	Gas @ 300°C

\*After C. E. Backus<sup>6</sup>

Table 2. Results of Kaplan Experiments\*

Emitter Temperature (°C)	Gas	Output Voltage (V)	Output Power (w/cm <sup>2</sup> )	Increase in Output Power (%)
1260	Cs	0.2	1.7	--
1260	Cs+ e	0.2	3.0	75
1370	Cs	0.3	5.8	--
1370	Cs+Xe	0.3	7.35	45

\* from Kaplan and Merzenich<sup>4</sup>

of the emitter, effectively decreasing the work function in the presence of cesium.

Several reports have been made since then which reverse the earlier conclusions.<sup>5,6</sup> The results of these reports are presented in Figs. 1, and 2. However none have considered the effect of helium upon the diode.

In this analysis the effects of helium and argon will be considered from the theoretical point of view. The considerations will include the effect of these gases upon the output due to changes in the plasma characteristics and the changes in heat transfer. The plasma changes will be reviewed using the point of view of a model developed by Backus,<sup>6</sup> and the heat transfer changes using the usual energy balance techniques.

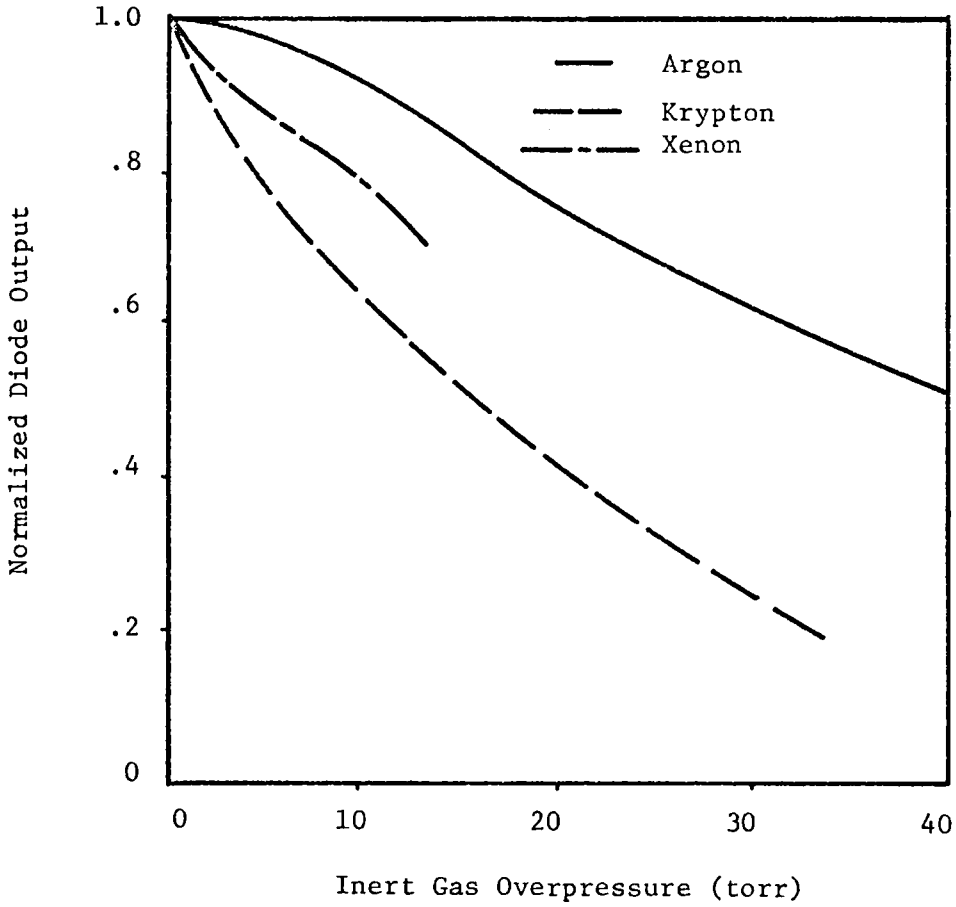


Fig. 1. The Effect of Inert Gas Overpressure on Diode Output.

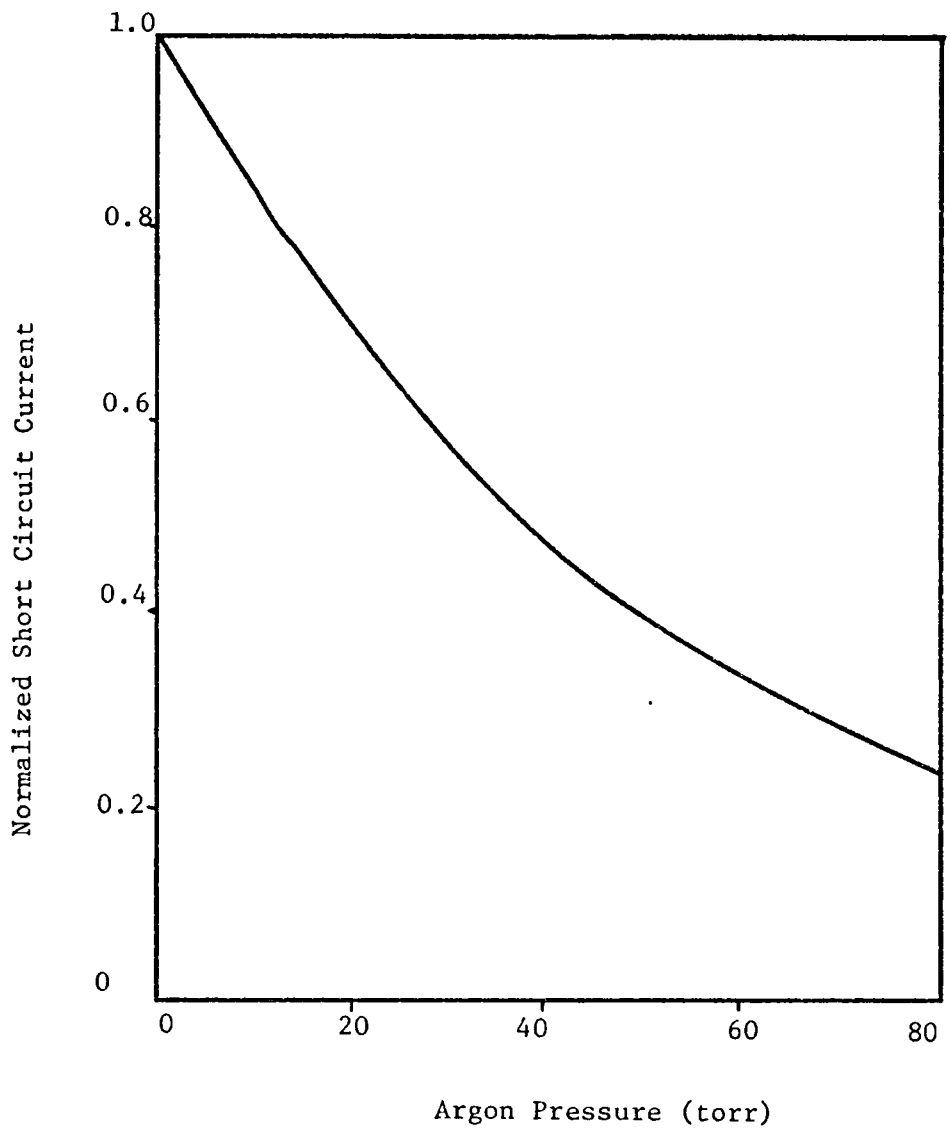


Fig. 2. Diode Output as Short Circuit Current versus Argon Overpressure.

## CHAPTER 2

### DIODE OPERATING CHARACTERISTICS

For the purpose of this analysis there are a number of parameters which must be determined in a self-consistent manner with the other parameters of interest. These parameters include the pressure of cesium, spacing, and their relation to emitter temperature and electron temperature. All of these are determined for the point at which the output is optimal.

To accomplish this optimization a model of the diode must be assumed, and the accompanying energy flow balances calculated.

For that purpose a number of models have been developed which relate the temperatures, pressures and spacing in thermionic diodes.

In this analysis the model to be assumed is presented in Rasor.<sup>7</sup>

The point of optimum performance occurs when the ion concentration exactly balances the emission, giving rise to a zero electric field at the emitter. The performance of diodes for various emitter voltage outputs is given in Fig. 3. Point A is the point of optimum practical operation.

The various regions of operation are noted in Fig. 3, however only the transition point will be considered here.

Because there is zero field at the emitter surface the saturation current is given by:

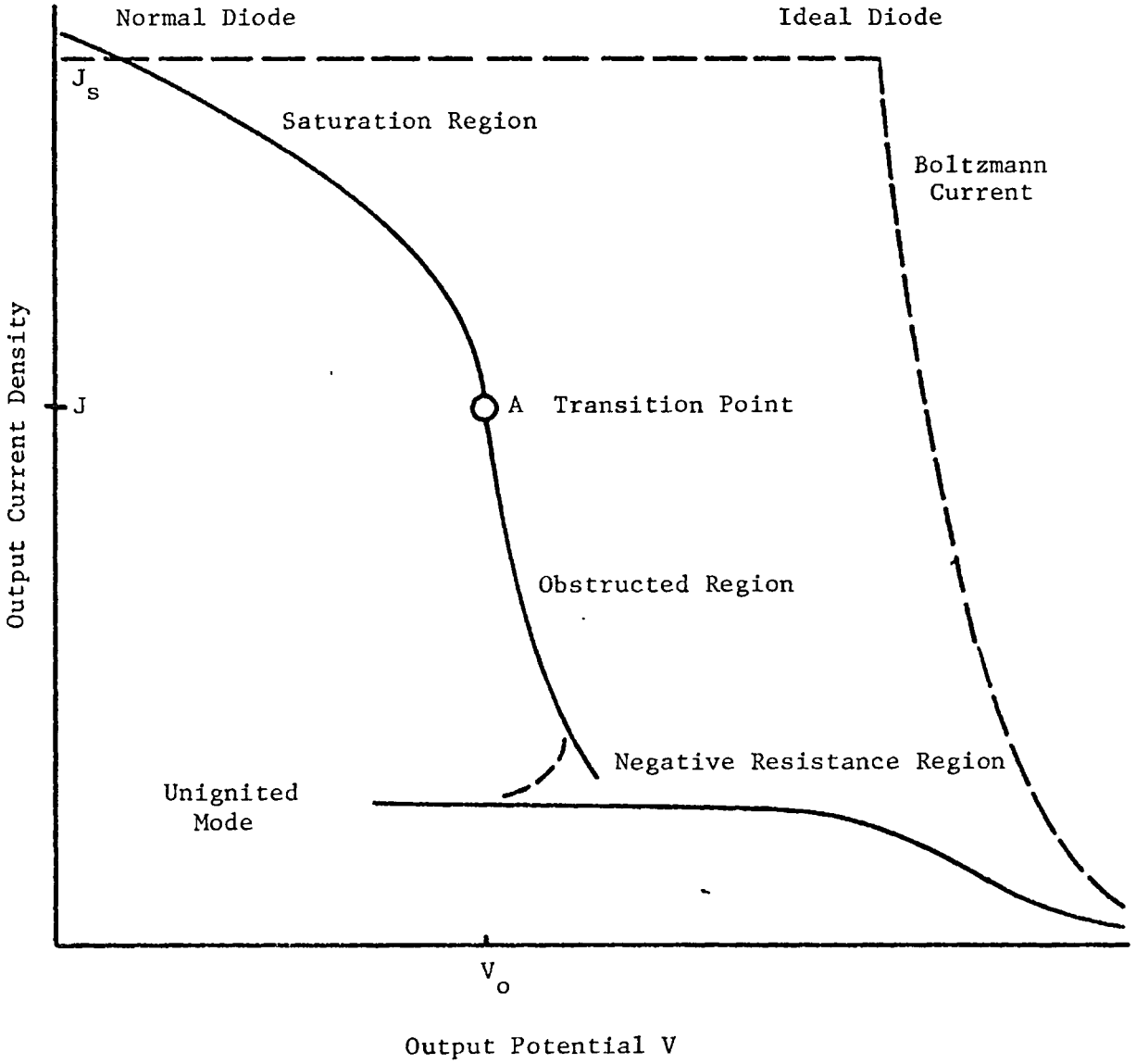


Fig. 3. IV Trace for Ideal and Normal Operation, after Rasor.

$$J_s = AT_E^2 \exp(-\phi_E/kT_E) \quad , \quad (2-1)$$

where

$\phi_E \equiv$  emitter work function (eV)

$T_E \equiv$  emitter temperature ( $^{\circ}$ K)

$A \equiv$  Richardson constant (120 amps/cm<sup>2</sup>  $^{\circ}$ K<sup>2</sup>)

$k \equiv$  Boltzmann constant ( $8.63 \cdot 10^{-5}$  eV/ $^{\circ}$ K) .

Figure 4 presents the electron motive diagram for operation at point A. It is from this motive diagram that the energy balance is drawn. The symbols used in Fig. 4 are defined as:

$\phi_E \equiv$  cesiated emitter work function (eV)

$eV_E \equiv$  emitter sheath voltage drop (eV)

$eV_C \equiv$  collector sheath voltage drop (eV)

$eV_d \equiv$  plasma voltage drop (eV)

$\phi_C \equiv$  cesiated collector work function (eV)

$eV_O \equiv$  output voltage (eV).

The motive diagram seems reasonable in view of the data presented by Bullis, Wiegand, and Bell.<sup>5</sup> It should be noted that the data do not agree with the large gradient of the electric field at the collector shown in Fig. 4. The stream of electrons from the emitter gains energy  $eV_E$  as it is accelerated into the potential well, thus the electrons at the emitter side of the plasma have temperature  $T_{eE} > T_E$ , and assuming the net electron energy lost within the plasma is negligible an energy balance will yield:

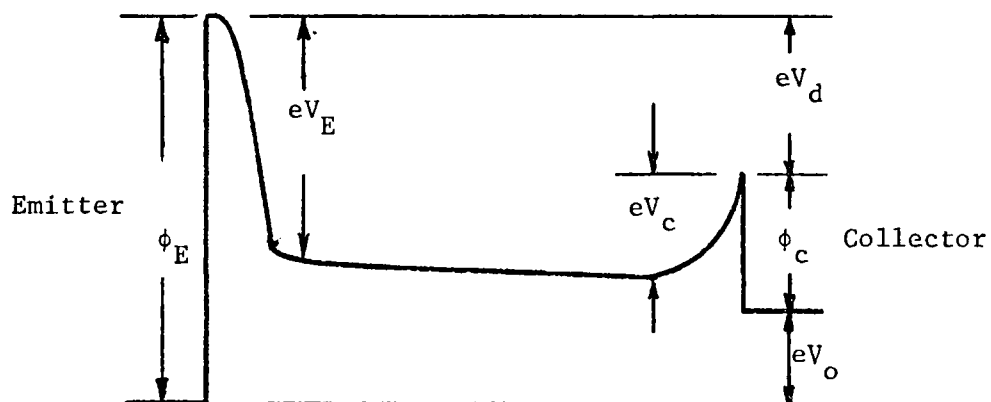


Fig. 4. Electron Motive Diagram Corresponding to the Transition Point.

$$2k T_{eE} = eV_c + 2k T_{ec} \quad . \quad (2-2)$$

The energy input to the plasma must equal that removed by the electrons in the collector current, and that in the reflected electron current. Thus, assuming negligible energy loss from the electrons to the plasma:

$$J_s (V_E + 2k T_E) = J(V_c + 2k T_{ec}) + (J_s - J) (V_E + 2k T_{eE}) \quad (2-3)$$

Since no heat is rejected and since negligible net work is performed by the electrons the second law of thermodynamics requires that the electrons conserve energy.<sup>7</sup> Thus:  $T_{ec} \approx T_E$ . Using this, and combining Eqs. (2-2) and (2-3) gives:

$$\frac{J}{J_s} = \frac{V_c}{V_E} \quad (2-4)$$

### Ion Balance

The ions in the interelectrode space which cancel the space charge the electrons' create, are themselves created by high energy electrons, and lost by diffusion to the electrodes and volume recombination.<sup>7</sup> The rate of ion production in a gas is:

$$v_i = n n_a d K_I \exp (-V_I/kT_e) \quad , \quad (2-5)$$

where

$v_i \equiv$  production rate of ion "i"

$n \equiv$  electron gas density

$n_a \equiv$  gas density

$d \equiv$  depth of gas column

$K_I \equiv$  ion generation coefficient

$V_I \equiv$  ionization potential.

$T_e \equiv$  electron temperature

$k \equiv$  Boltzmann constant.

The rate at which ions diffuse from the plasma to the electrodes is given by:<sup>7</sup>

$$\mu_i = K_D n_i \frac{\lambda}{d} , \quad (2-6)$$

where

$\mu_i \equiv$  diffusion of species  $i$

$K_D \equiv$  ion loss coefficient

$n_i \equiv$  ion density

$\lambda \equiv$  mean-free-path

$d \equiv$  diffusion length (electrode spacing).

By combining Eqs. (2-5) and (2-6) and equating sources and sinks, then:

$$T_{eE} = V_I / 2 \ln (B p d) , \quad (2-7)$$

where  $B$  is the ion balance coefficient, and is equal to 40 (torr-mil.)<sup>-1</sup>.<sup>7</sup>

It should be pointed out that the dominant ionization mechanism in the ignited mode is that of volume ionization. The high energy electrons necessary for the generation of the ions are indeed present as can be seen by inspecting Reichelt's data.<sup>8</sup> That this, the volume ionization mechanism, is the dominant mechanism, is discussed by Talaat.<sup>9</sup> It is pointed out therein that the ignited mode operation depends

upon the electron temperature being raised sufficiently high by acceleration in the emitter sheath to cause a large number of ionizations. This increase in ion density causes the electric field at the emitter to become larger. Thus the emitter sheath voltage drop is not only present, as shown in Fig. 5, but necessary for operation in the ignited mode.

### Electron Transport

The transport of electrons from the emitter is treated as a neutral, field-free plasma, bounded by emitter and collector sheaths of height  $V_E$  and  $V_C$  respectively, and since no significant source or sink of electrons exists in the plasma,<sup>10</sup>

$$\frac{d^2n}{dx^2} = 0 \quad , \quad (2-8)$$

where  $n$  is the density of electrons at distance  $x$  from the emitter.

It is shown in Appendix A that the difference of saturation current  $J_s$  and output current  $J$  is given by:

$$J_s - J = \exp(-V_E/kT_{eE}) \left[ \frac{3}{4} \frac{d}{\lambda} J + R J \right]$$

with  $R = \exp(V_C/kT_{eC}) - 1$  (2-9)

Equations (2-2), (2-4), (2-7), and (2-9) can be combined<sup>7</sup> to calculate the electron temperature  $T_e$ , current density  $J$ , and the arc drop across the plasma  $V_d$  as a function of cesium pressure  $p$ , spacing  $d$ , emitter temperature  $T_E$ , and emitter work function  $\phi_E$ . Figures 6 and 7 present the results obtained by Rasor.<sup>7</sup>

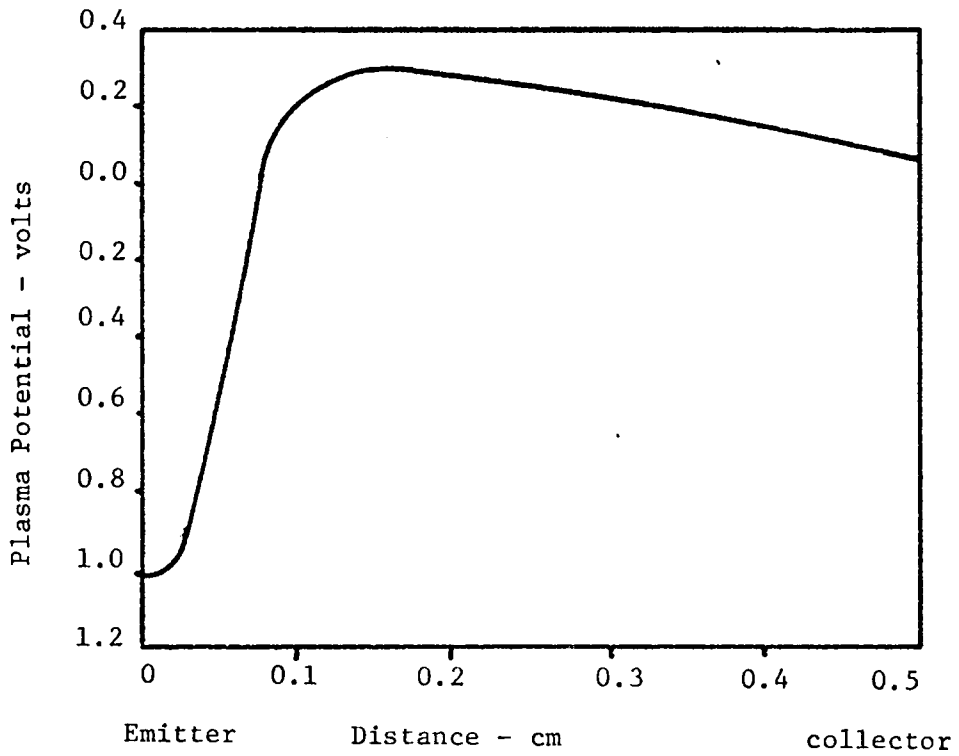


Fig. 5. Variation of Plasma Potential with Position.

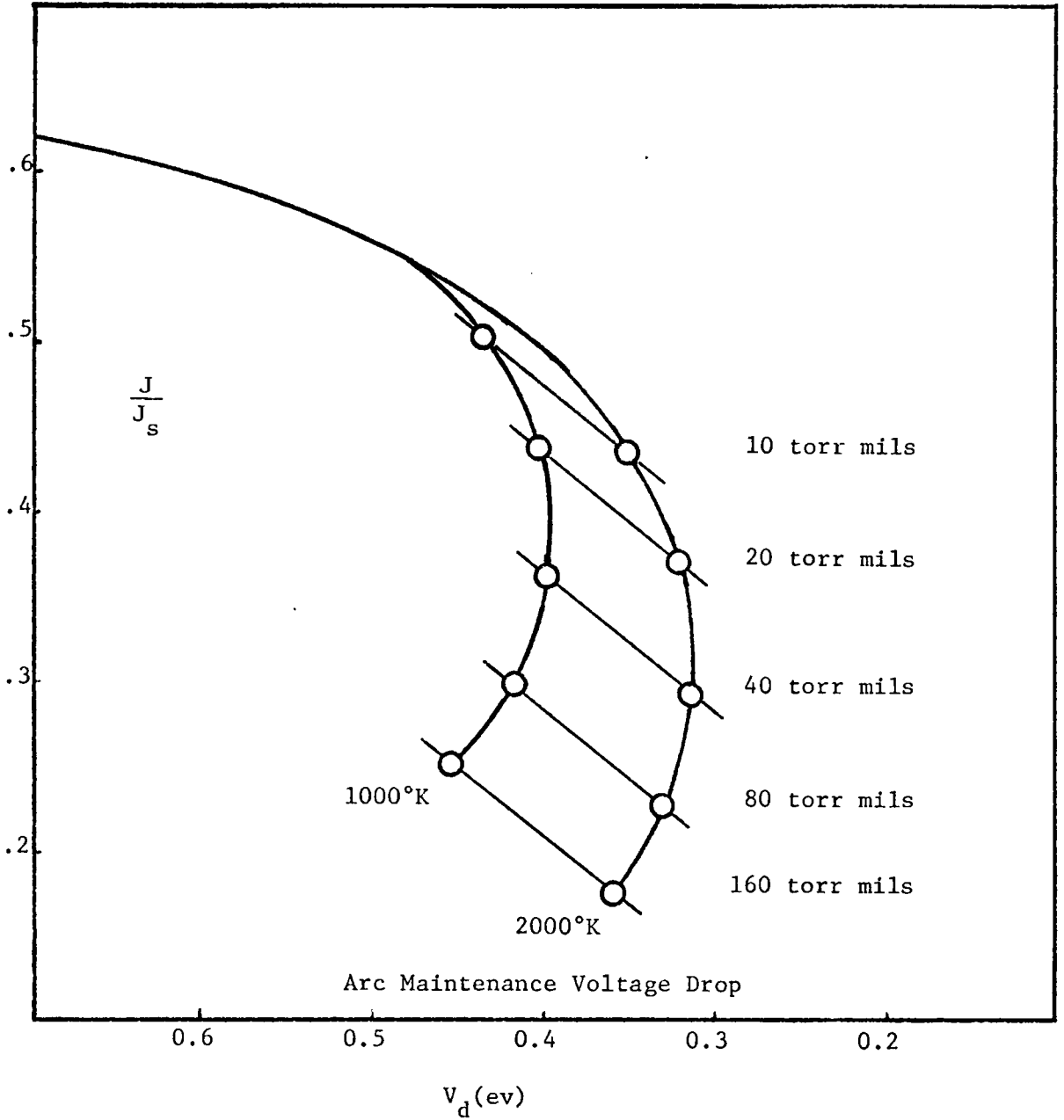


Fig. 6. Dependence of Arc Maintenance Drop  $V_d$  upon Transition Current Density  $J$ , on Emitter Temperature and the Pressure-Spacing Product

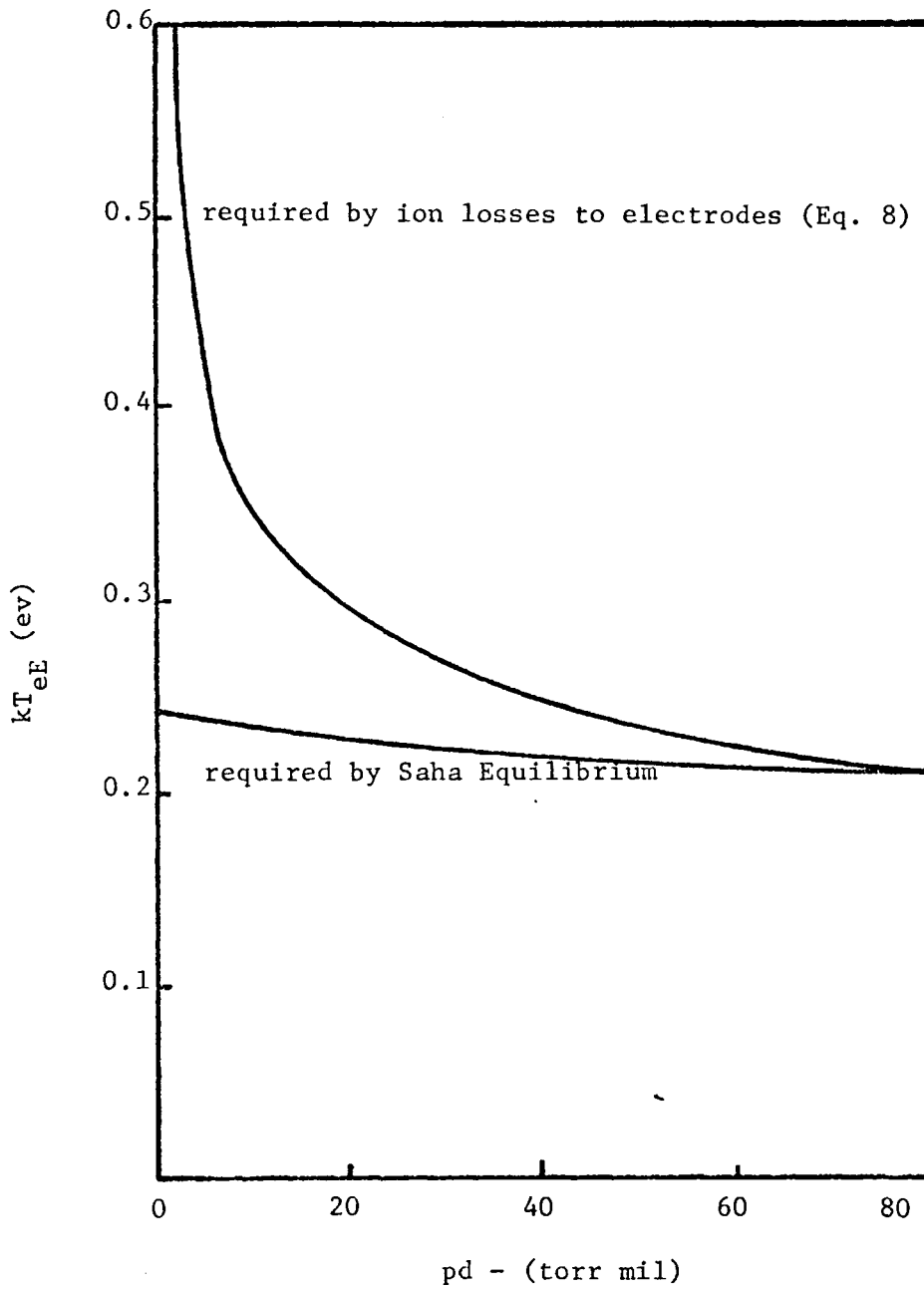


Fig. 7. Dependence of Electron Temperature  $T_{eE}$  at Emitter Edge of Plasma on Pressure-Spacing Product  $pd$  in the Ignited Mode

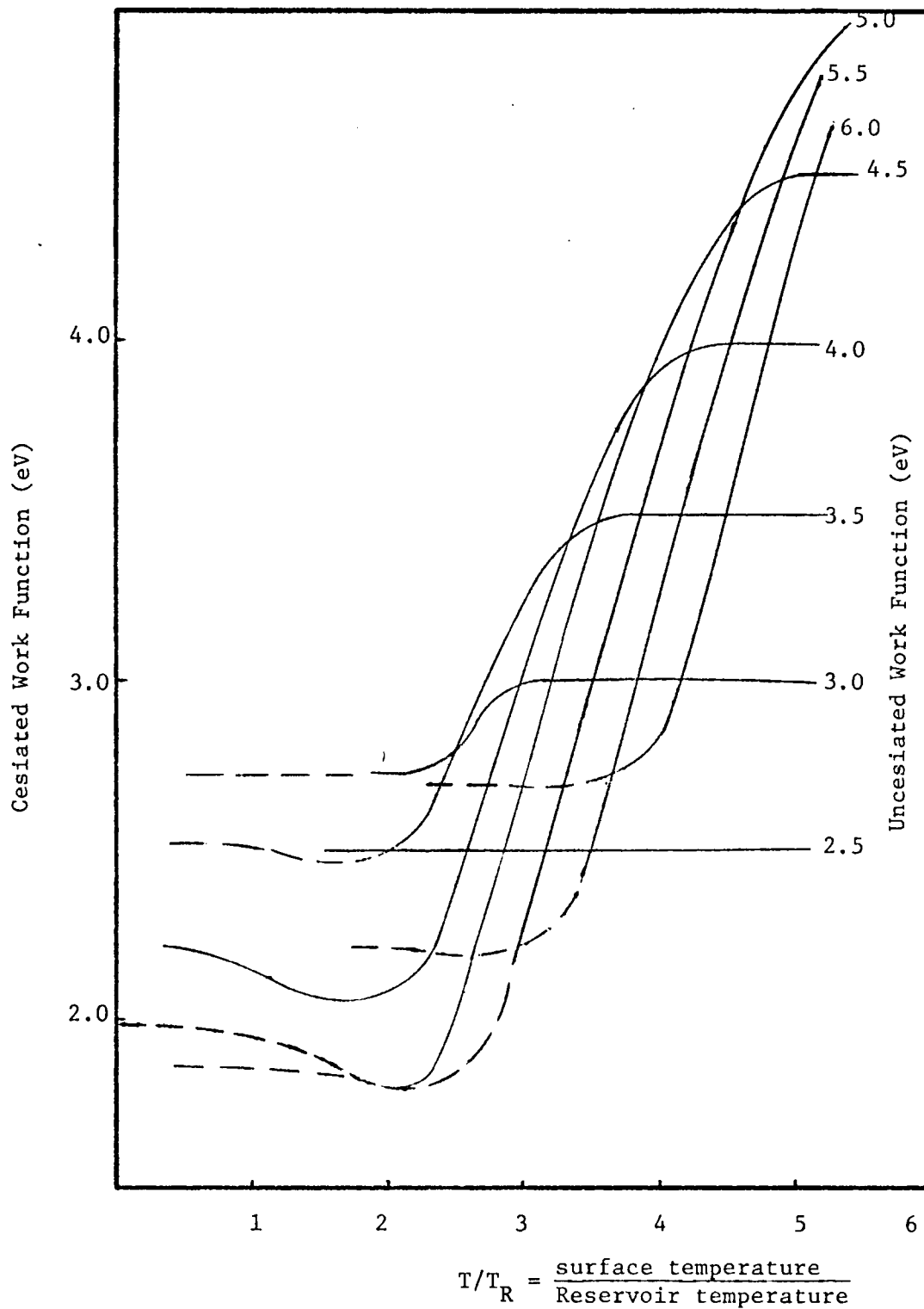


Fig. 8. Work Function of Surface Refluxed with Cesium Vapor

Assuming an emitter temperature of  $2000^{\circ}\text{K}$  made of tungsten, and a collector of nickel operating at  $1000^{\circ}\text{K}$ , and assuming a pressure-spacing product of 20 (torr-mil), then the arc drop voltage  $V_d \approx 0.32$  volts and  $J/J_s \approx 0.37$ .

Stipulating the diode output as  $J=10$  amps/cm<sup>2</sup> sets  $J_s=37$  amps/cm<sup>2</sup>, and the emitter work function at  $\phi_E=2.81$  eV.

Assuming the tungsten surface had a work function of 4.5 eV before being cesiated, then the required reservoir to emitter temperature ratio, as given by Fig. 8 is  $T_E/T_R \approx 3.1$  or a cesium reservoir temperature of  $645^{\circ}\text{K}$ . This corresponds to a cesium pressure of  $\sim 9.6$  torr. Thus the necessary spacing for  $pd=20$  mil-torr is  $d \approx 2.08$  mils. This is a close spaced diode, but it yields a self-consistent model.

Based on the assumption that volume recombination is of small importance in the loss of ions in the plasma, the energy of the electrons at the emitter is predicted (Fig. 7) to be  $\sim 0.296$  eV. This corresponds to a temperature of  $3,920^{\circ}\text{K}$ .

It will be assumed the nickel collector is operating at  $1000^{\circ}\text{K}$ , and therefore has a work function  $\phi_c \sim 1.81$  eV.

It should be noted that a  $p\lambda$  product of 2 mil-torr was assumed in the calculation.<sup>7</sup> With a cesium pressure of 9.6 torr the mean-free-path is  $\sim 5.10^4$  cm, which corresponds to a  $p\lambda \approx 2$  mil torr. From Fig. 6 it can be seen that the predicted voltage drop is  $\sim 0.32$  V. Thus the output voltage, neglecting IR losses is 0.68 volts, or a power of 6.8 watts/cm<sup>2</sup>.

## CHAPTER 3

### ELECTRON DIFFUSION CHANGES

The introduction of inert gases into the interelectrode spacing causes an increase in the number of scattering centers present in the plasma. The distribution of particles in the diode space can be analyzed for output changes if the terms of interaction type may be separated. This is not the case in high density fields or fluids.<sup>11</sup> Thus the distribution is given by:

$$\frac{\partial f}{\partial r} = -\omega \frac{\partial f}{\partial r} - \gamma \frac{\partial f}{\partial \omega} \quad (3-1)$$

where the first term:

$$-\omega \frac{\partial f}{\partial r}$$

expresses the influence of the diffusion phenomenon. ( $\omega$ ) is the velocity of the particles, and  $\frac{\partial f}{\partial r}$  is the gradient of the distribution with respect to position. The second term:

$$-\gamma \frac{\partial f}{\partial \omega}$$

expresses the action of applied forces; i.e., for particles carrying charge  $q$  and in an applied field,  $E$ , then:

$$\gamma = \frac{qE}{m}$$

where  $m$  is the mass of the particle.

The quantity of interest here is the flow of electrons and ions through the plasma of the interelectrode space. Assuming that the gas is weakly ionized, the electron collisions can be ignored, and the gas is considered homogeneous and infinite. In the absence of magnetic fields, it has been shown<sup>11,12</sup> that the Boltzmann equation for particle current flow becomes:

$$\begin{aligned}\Gamma_e &= -\nabla(D_e n_e) - \mu_e E n_e \\ \Gamma_i &= -\nabla(D_i n_i) + \mu_i E n_i\end{aligned}\quad (3-2)$$

for electrons and ions respectively.

For purposes of measurement of the effect of inert gases the ion and electron currents are measured jointly, however, for the purpose of calculation they are considered separately.

If the spacing is much larger than the electron or ion mean-free-path then the mobility and diffusion coefficients are given by:

$$\begin{aligned}\mu_e &= \frac{q_e}{m_e \langle v_e \rangle} \quad , \\ \mu_i &= \frac{q_i}{m_i \langle v_i \rangle}\end{aligned}\quad (3-3)$$

and

$$\begin{aligned}D_e &= \frac{kT_e}{m_e \langle v_e \rangle} \quad , \\ D_i &= \frac{kT_i}{m_i \langle v_i \rangle} \quad .\end{aligned}\quad (3-4)$$

Using the above and Eq. (3-2),

$$\Gamma_e = -\frac{n_e q_e E}{m_e \langle v_e \rangle} - \frac{kT_e}{m_e \langle v_e \rangle} \nabla n_e \quad (3-5)$$

and

$$\Gamma_i = \frac{n_i q_i E}{m_i \langle \nu_i \rangle} - \frac{k T_i}{m_i \langle \nu_i \rangle} \bar{\nu} n_i. \quad (3-6)$$

where the subscripts "e" and "i" refer to electron and ion parameters respectively and:

$\Gamma$   $\equiv$  particle current

$n$   $\equiv$  particle density

$q$   $\equiv$  particle charge

$m$   $\equiv$  particle mass

$k$   $\equiv$  Boltzmann constant

$E$   $\equiv$  electric field

$T$   $\equiv$  particle temperature

$\langle \nu \rangle$   $\equiv$  average collision frequency.

The average collision frequency can be expressed as follows:

$$\langle \nu \rangle = \sigma_s N v, \quad ,$$

where  $\sigma_s$   $\equiv$  scattering cross-section.

$N$   $\equiv$  density of scattering centers

$v$   $\equiv$  average particle velocity.

The equation relating output to the particle currents is:

$$J = \Gamma_e q_e - \Gamma_i q_i. \quad (3-7)$$

Thereby, using Eqs. (3-5) and (3-6),

$$J_e = \frac{q_e^2}{m_e \langle v_e \rangle} n_e \bar{E} + \frac{q_e k T_e}{m_e \langle v_e \rangle} \nabla n_e ,$$

and

$$J_i = - \frac{q_i^2}{m_i \langle v_i \rangle} n_i \bar{E} + \frac{k T_i}{m_i \langle v_i \rangle} \nabla n_i . \quad (3-8)$$

### Evaluation

In considering the application of the above theory to the effect of an inert gas upon diode output several assumptions applicable to both particle currents, must be made. They are:

1. The mean-free-path of the particle is small compared to the electrode spacing
2. A Maxwellian distribution of particle velocities is achieved
3. The inert gas has no effect upon the surface emission characteristics.

The evaluation will be carried out by considering small perturbations on the equilibrium system. Thus it should be kept in mind that the results are valid only for linear perturbations to the operating system.

### Ion Current

The output of the diode due to ion current will be small compared to the electron current because the ion mobility and diffusion are several orders of magnitude smaller than the same electron properties as seen in Eq. (3-9).

$$\left| \mu_e / \mu_i \right| = D_e / D_i = (m_i / m_e)^{1/2} \quad (3-9)$$

### Electron Current

The effect of increased inert gas pressure on the electron current will require the evaluation of several parameters.

The electron temperature will be taken to be the average of the emitter side electron temperature and the collector side electron temperature. Assuming that  $T_{ec} \approx T_E$ ,<sup>7</sup> then the average,  $T_e$  equals 2860°K ( $\sim 0.497\sqrt{\text{volts}}$ ).

The ratio of  $\sqrt{n_e}/n_e$  is taken from Fig. 9 to be  $\sim 6.0$  for electrons at the collector surface. The ratio is assumed to be constant over the range of operation, provided the mode of operation does not change.

The electric field at the collector edge is taken from Fig. 5 to be a retarding field of  $\sim 0.8$  volts/cm, and constant.

The helium and argon cross-sections are presented in Fig. 10. The minimum observed in the cross-section of argon is due to the Ramsauer effect. The energies of interest fall between  $0.4-0.5\sqrt{\text{volts}}$ .

The change of output with inert gas pressure may be found by taking the ratio of electron current  $\Gamma_e$  to the unperturbed current  $\Gamma_{eo}$ . Thus after some manipulation Eq. (3-5) becomes:

$$\frac{\Gamma_e}{\Gamma_{eo}} = \frac{n_e N_o v_{eo} \sigma_o}{n_{eo} N v_e \sigma} \left[ \frac{-\frac{q_e E}{k} - \frac{\sqrt{n_e}}{n_e} T_e}{-\frac{q_e E}{k} - \frac{\sqrt{n_{eo}}}{n_{eo}} T_{eo}} \right] \quad (3-10)$$

where

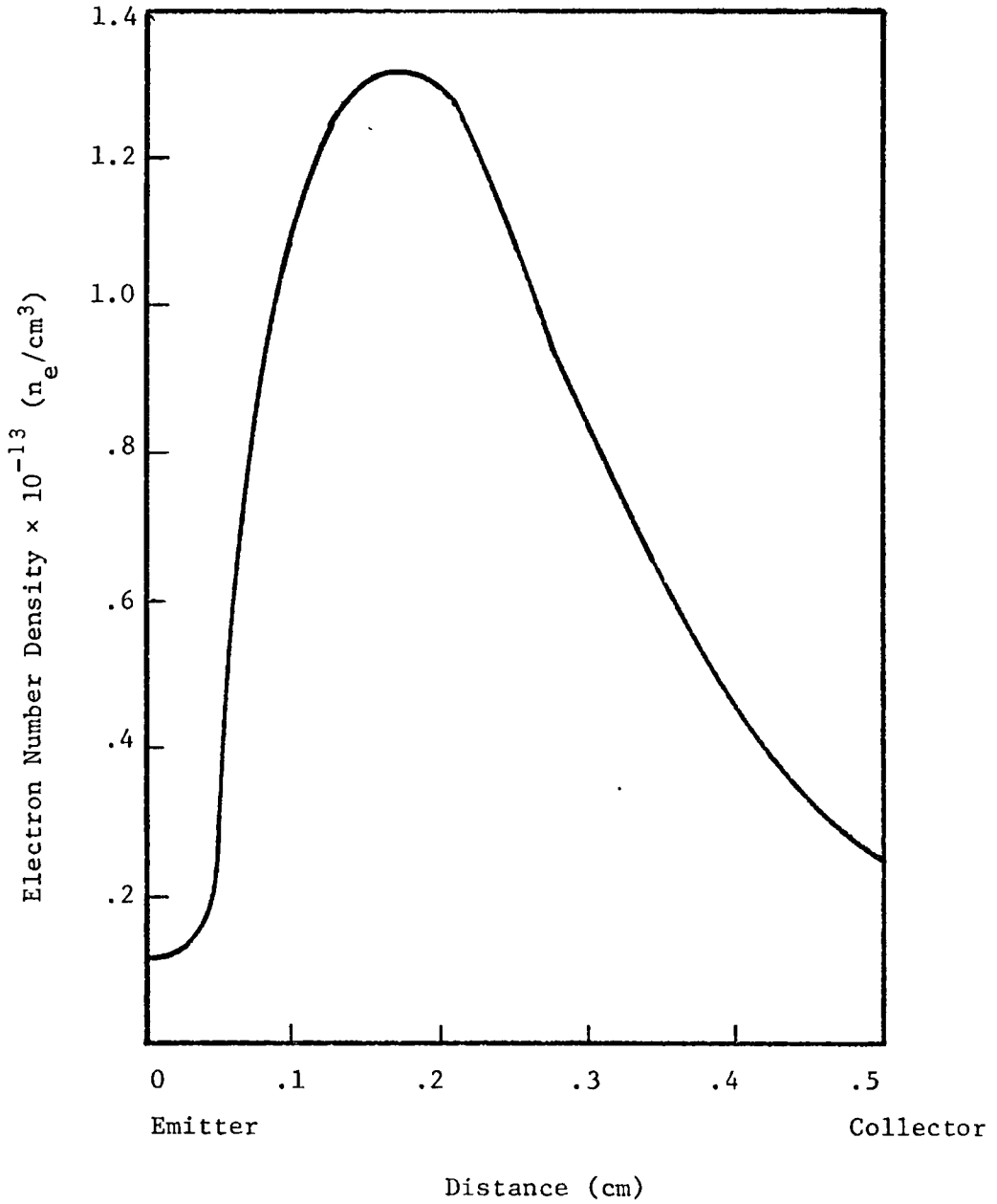


Fig. 9. Electron Density versus Position

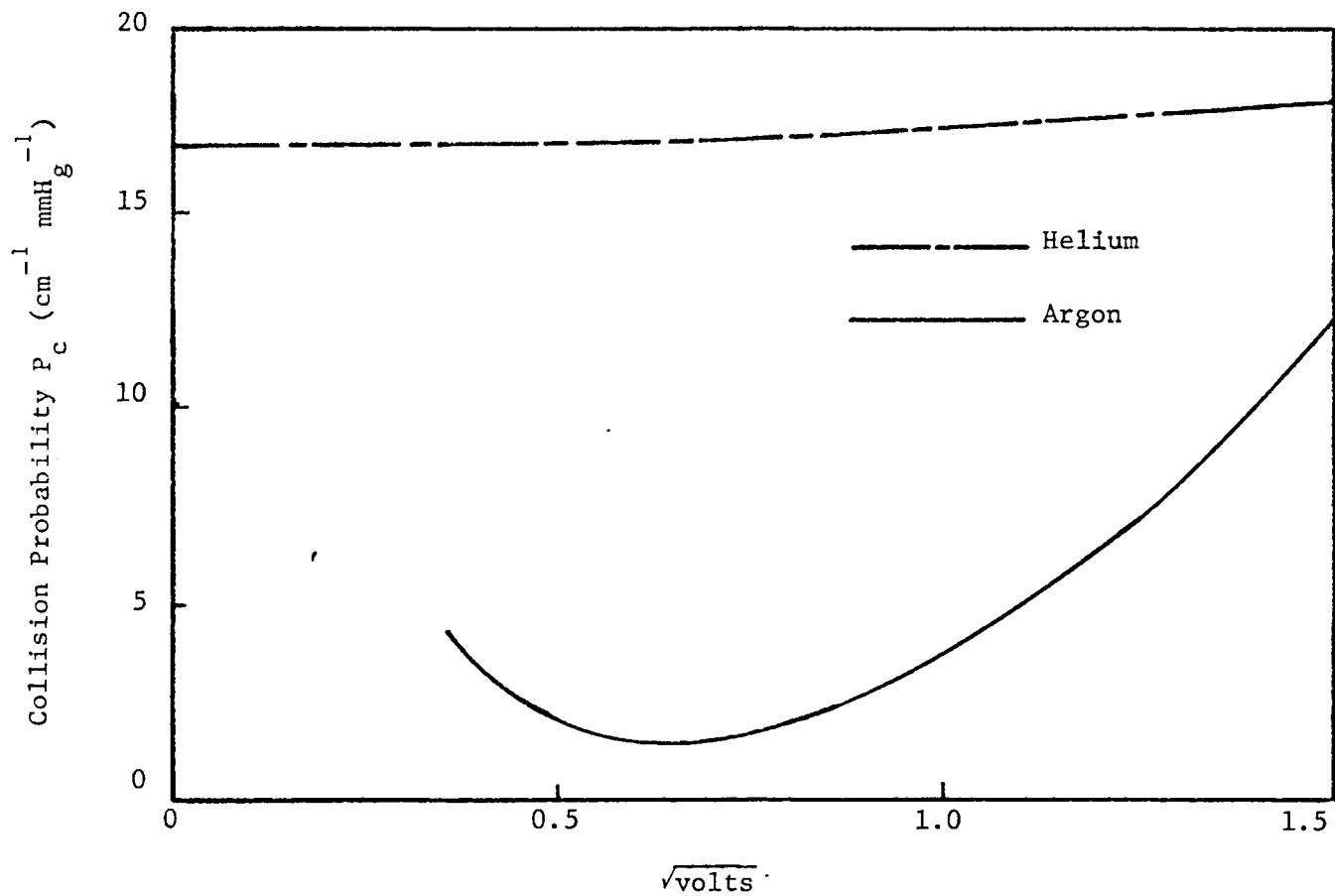


Fig. 10. Collision Probability ( $\text{cm-mmHg}$ )<sup>-1</sup> versus Electron Energy ( $\sqrt{\text{volts}}$ )

$n_e \equiv$  electron density ( $ne/cm^3$ )

$N \equiv$  density of scattering centers ( $/cm^3$ )

$v_e \equiv$  electron velocity (cm/sec)

$J \equiv$  electron-gas cross-section ( $cm^{-1} - mmHg^{-1}$ )

$T_e \equiv$  electron temperature (eV).

The subscript zero signifies the initial condition.

The change in electron density with pressure is taken from Bullis et al,<sup>5</sup> and is given in Fig. 11. The effect of helium is computed by assuming the slope is proportional to the cross-sections of the gas involved.

The changes in electron temperature are also taken to be proportional to the cross-sections of the gases involved, and thus the helium and argon data in Fig. 12 are calculated from the data for krypton.<sup>6</sup>

The changes in cross-section with increasing inert gas pressure is calculated by defining:

$$\sigma = \frac{N_1 \sigma_1 + N_2 \sigma_2}{N_1 + N_2}$$

where

$N_1, N_2 \equiv$  density of atoms of type 1,2 ( $N/cm^3$ ).

$\sigma_1, \sigma_2 \equiv$  cross-section of electron-gas interaction ( $cm^{-1} - mmHg^{-1}$ )

The cross-sections used to make this calculation are presented in Figs. 10 and 13. The results are given in Fig. 14.

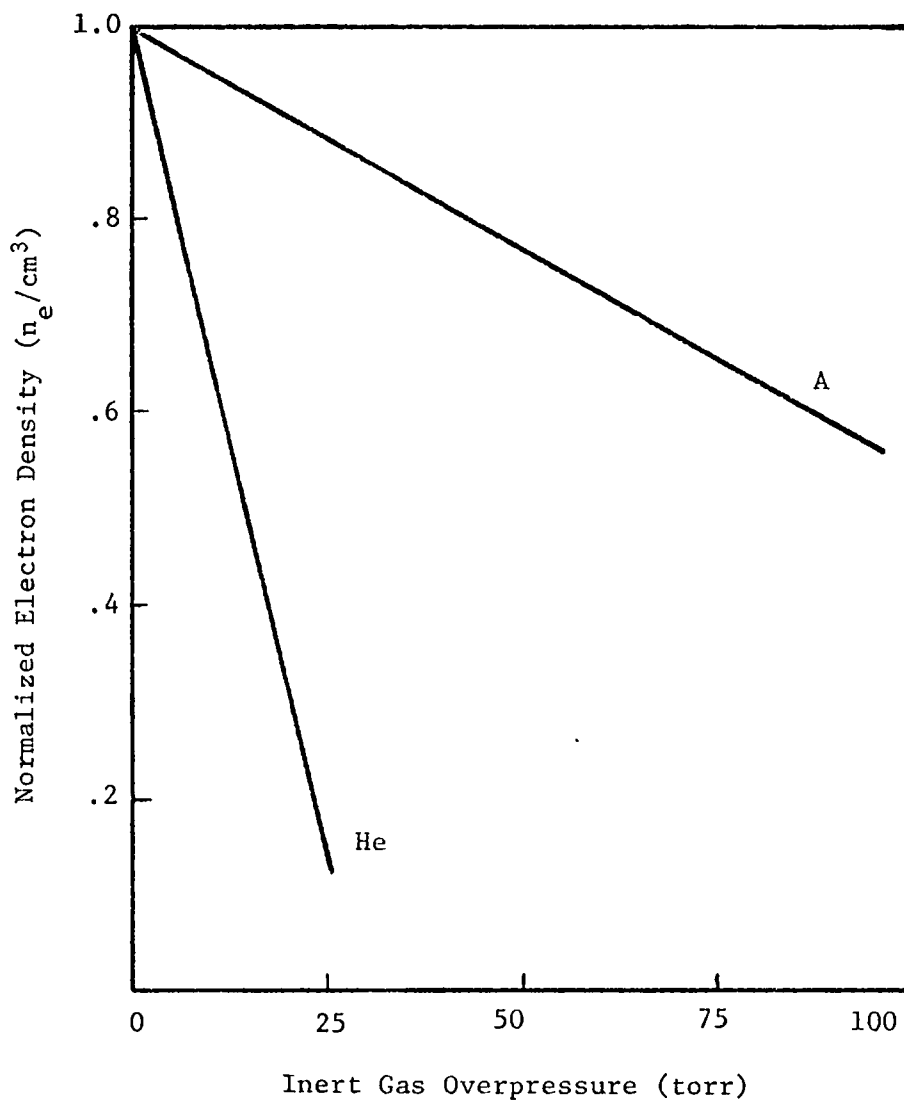


Fig. 11. Normalized Electron Density versus Inert Gas Overpressure

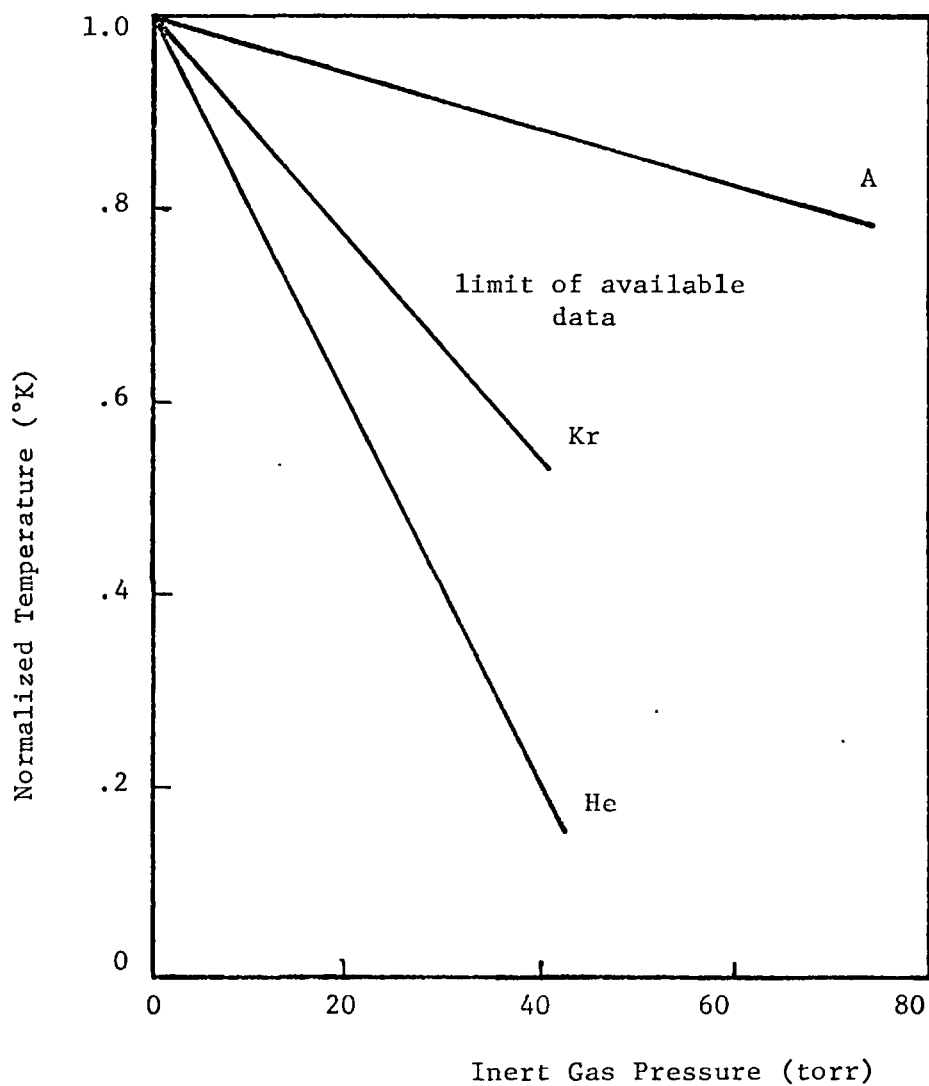


Fig. 12. Normalized Temperature versus Inert Gas Pressure (torr)

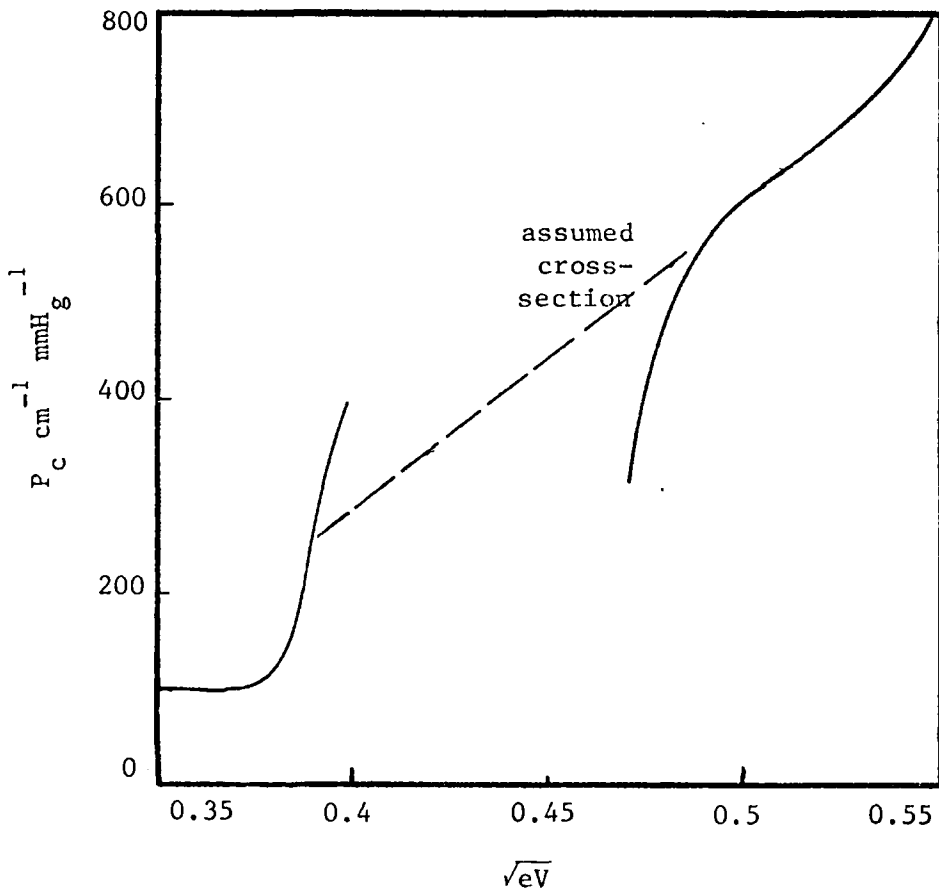


Fig. 13. Cesium Cross-Section

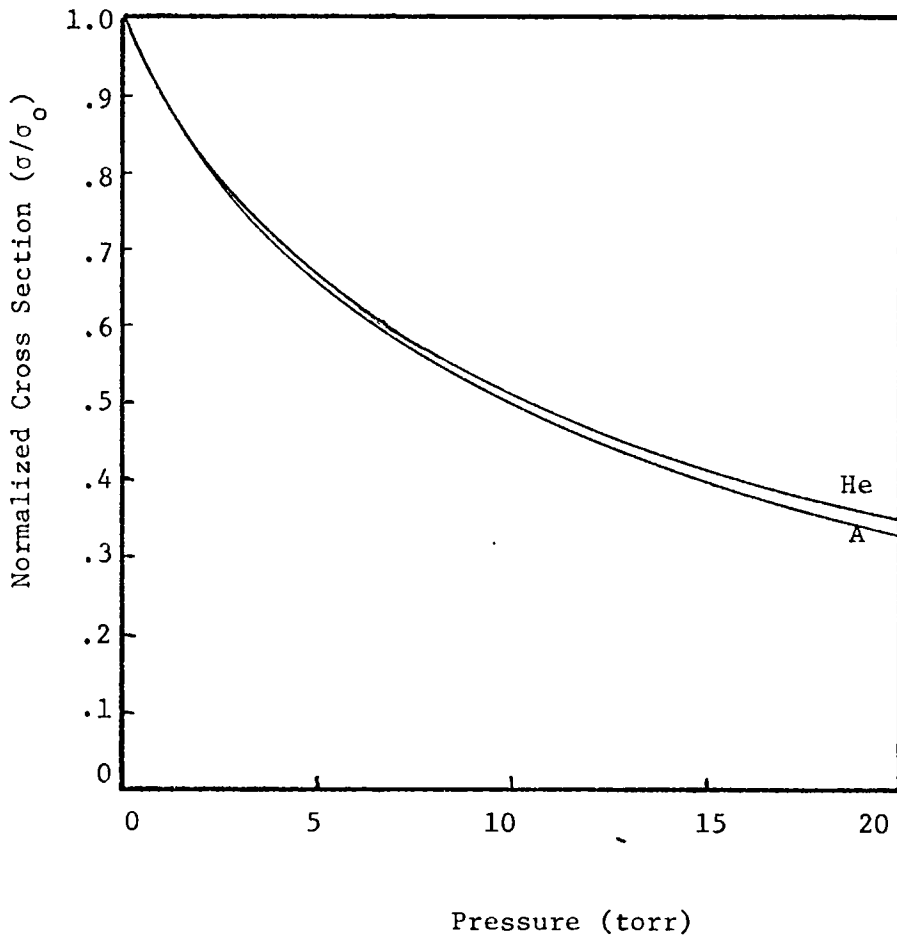


Fig. 14. Normalized Cross-Section versus Inert Gas Pressure (torr)

The cesium cross-section was taken from Flavin and Meyer<sup>13</sup> and seems to represent the data available at this time.<sup>14</sup>

The velocity changes are taken from the temperature data and are presented in Fig. 15.

All of the approximations for electron density and temperature changes are first order approximations of the relative effects approximations are not considered reliable above 15-20 torr, where the perturbations cease to be small. Combining the data as prescribed in Eq. (3-10), the change in particle current may be calculated. This change is presented in Fig. 16.

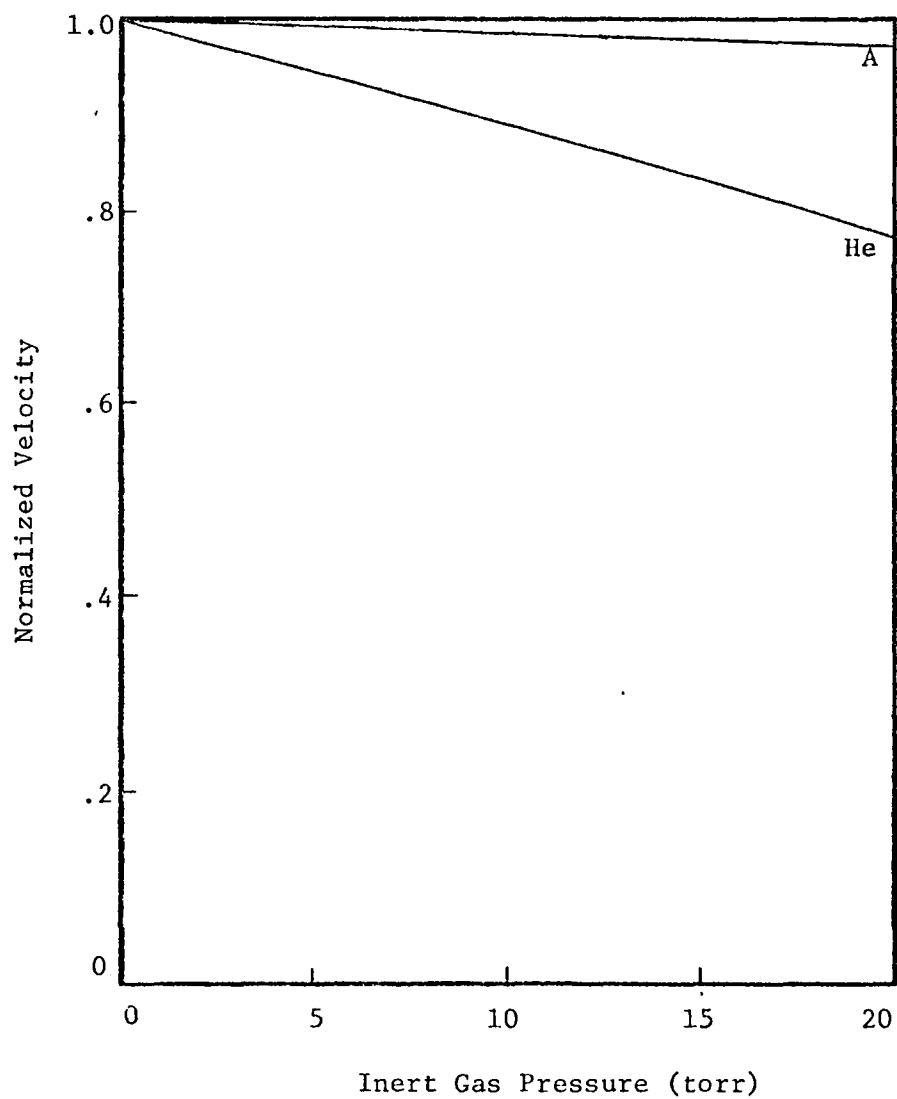


Fig. 15. Normalized Velocity versus Inert Gas Pressure

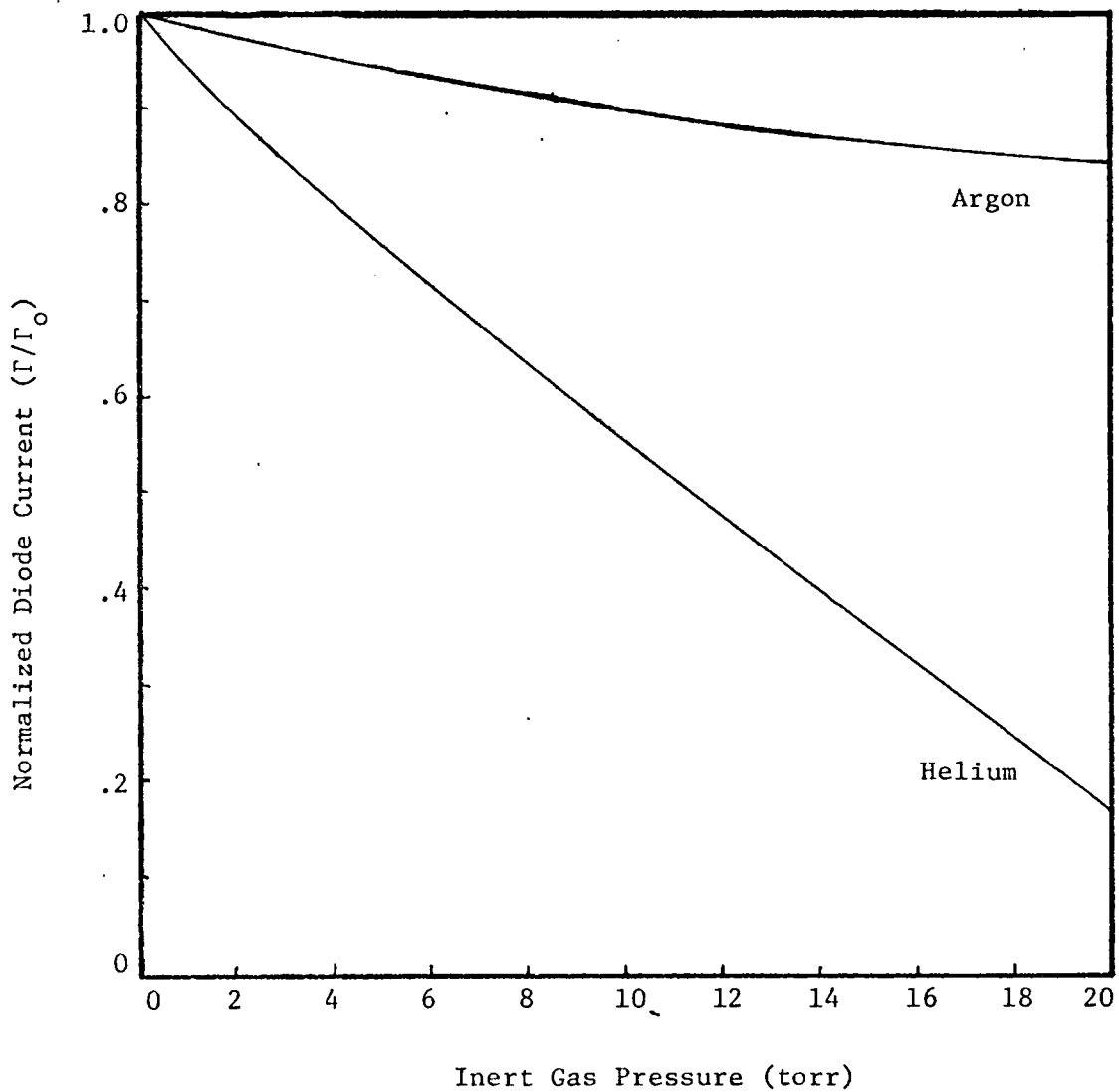


Fig. 16. Normalized Diode Current versus Inert Gas Pressure

## CHAPTER 4

### ENERGY TRANSPORT

The energy transfer between the emitter and collector will be analyzed assuming the emitter and collector have constant temperatures. The case of constant heat flux is outlined in Appendix C.

Having set the emitter and collector temperatures, the heat transfer due to the mechanisms of inert gas conduction, radiative heat transfer, cesium conduction, and electron energy transport may be analyzed for the heat flow due to each mechanism. Having calculated the heat flow the efficiency of the cell may be calculated using the information presented in Chapter 2. Assuming the efficiency of the cell is constant, the effect of the net change in energy transport will be evaluated.

#### Cesium Energy Transport

Cesium in the interelectrode space will transfer heat by conduction only, and therefore the resistivity coefficient is given by:

$$R_{es} = \frac{L}{A k} ,$$

where  $L$  is the spacing,  $A$  the area of transfer, and  $k$  the conductivity coefficient.

The inverse resistivity coefficient,<sup>15</sup> (conductivity) is given in Fig. 17.

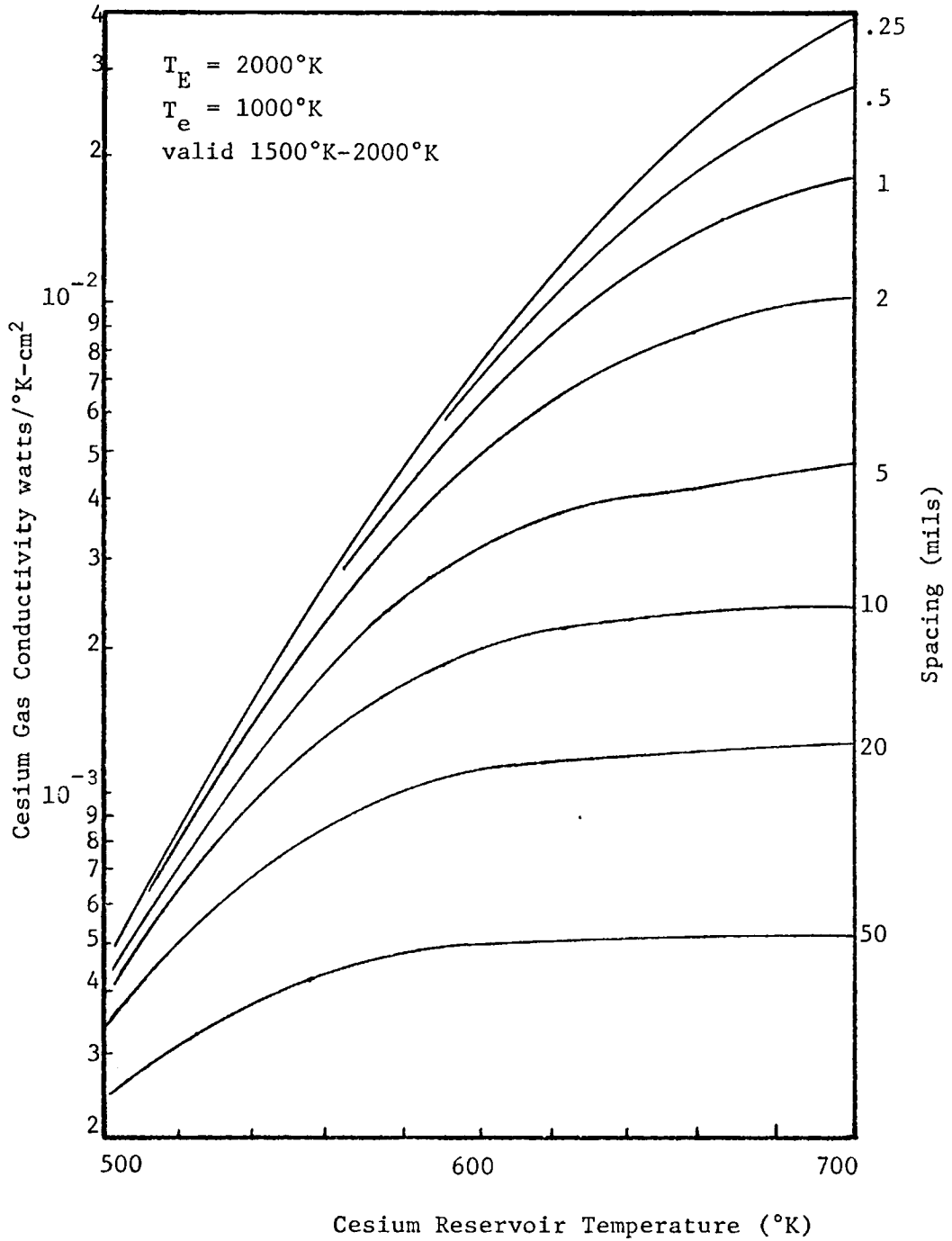


Fig. 17. Gas Conductivity (watts/ $^\circ\text{K}\text{-cm}^2$ ) versus Cesium Reservoir Temperature ( $^\circ\text{K}$ )

Once the diode spacing and reservoir temperature are set the amount of energy transport across the gap is easily found.

As calculated in Chapter 2 the gap  $d \approx 2.08$  mils, therefore for the conditions stated the net transfer is 8.15 watts/cm<sup>2</sup>.

### Radiative Energy Transport

The emitter, operating at 2000°K, will radiate a large amount of energy to the collector, at 1000°K.

Assuming a highly polished emitter and collector, specular reflection will govern the net transfer of energy.

A common simplification in the evaluation of the emissivities has been used to evaluate the radiative heat transport between tungsten and nickel.<sup>16</sup> The equation for the net energy transfer per unit area,  $q_R$ , is given by:

$$q_R = \sigma \left[ \frac{T_E^4 \epsilon_E}{\frac{1}{\epsilon_E(T_E)} + \frac{1}{\epsilon_C(T^*)} - 1} - \frac{T_C^4 \epsilon_C}{\frac{1}{\epsilon_E(T^*)} + \frac{1}{\epsilon_C(T_C)} - 1} \right] \quad (4-1)$$

where

$q_R \equiv$  energy transport (watts/cm<sup>2</sup>)

$\sigma \equiv$  Stephan-Boltzmann constant  
 $= 5.67 \cdot 10^{-12}$  watts/°K<sup>4</sup> cm<sup>2</sup>

$T_E \equiv$  emitter temperature (°K)

$T_C \equiv$  collector temperature (°K)

$\epsilon_E(T_o) \equiv$  emissivity of the emitter at temperature  $T_o$

$\epsilon_C(T_o) \equiv$  emissivity of the collector at temperature  $T_o$

$$T^* = \sqrt{T_E T_C} .$$

Using Eq. (4-1) the radiative heat transfer was calculated,<sup>16</sup> and the results are presented in Fig. 18.

For the conditions stated the net transfer is 11 watts/cm<sup>2</sup>.

### Electron Energy Transport

Electron energy transport across the plasma to the collector is going to be reduced due to the drop in electron current output. Because the emitter has a constant temperature, the saturation current will not change. Thus, by conservation of electron current there is an increased current returning to the emitter.

The effect of this larger return current may be analyzed in an approximate way by realizing that the increased albedo of the plasma is in fact an incremental increase in the effective source.

For small perturbations, such that the emitter temperature stays constant, the effect of this change may be analyzed by assuming a constant efficiency for the diode. This can be expressed as:

$$\beta = \frac{J V_o}{q''} \tag{4-2}$$

where

$\beta =$  efficiency

$J =$  current output per unit area (amps/cm<sup>2</sup>)

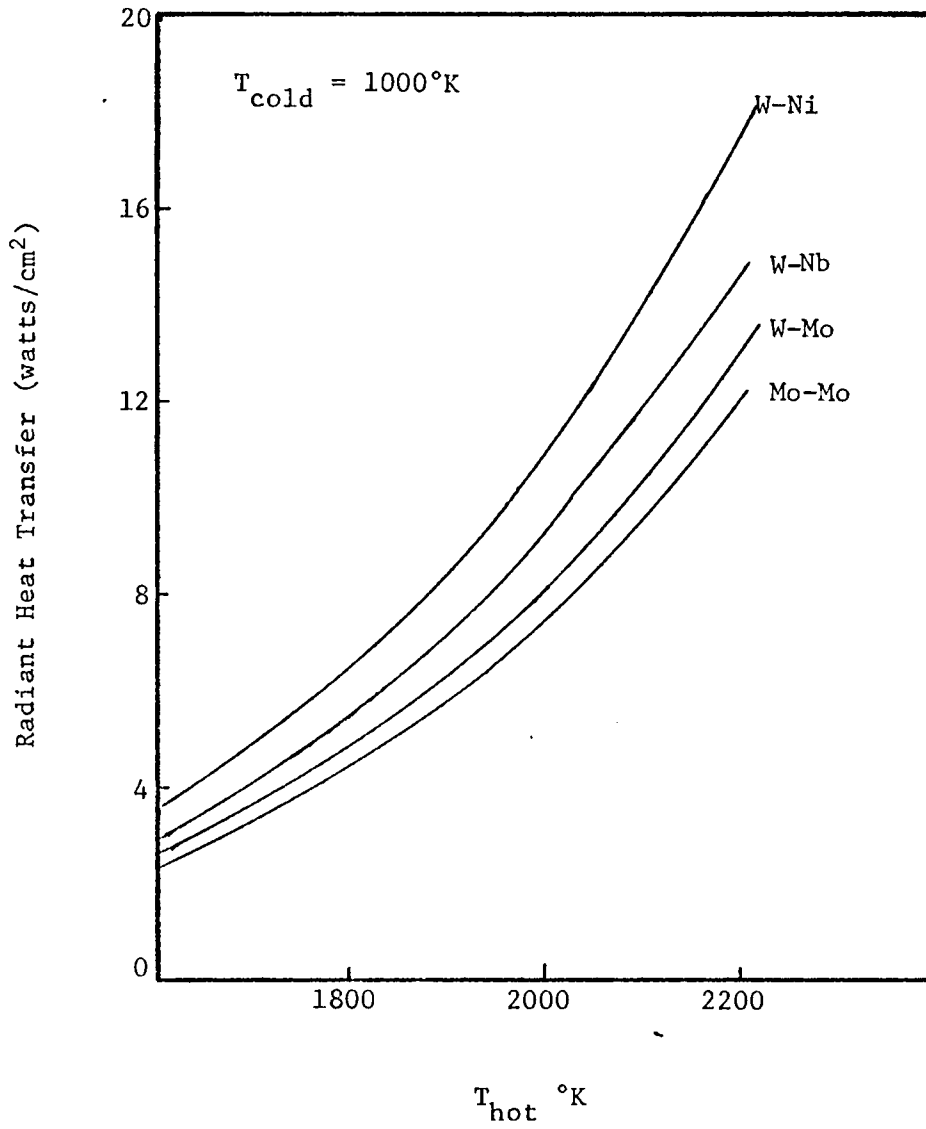


Fig. 18. Radiative Net Heat Transfer versus Hot Surface Temperature for Several Materials

$V_o \equiv$  output voltage (volts)

$q'' \equiv$  heat source per unit area (watts/cm<sup>2</sup>) .

Figure 19 gives the physical representation of the albedo,  $\eta$ .

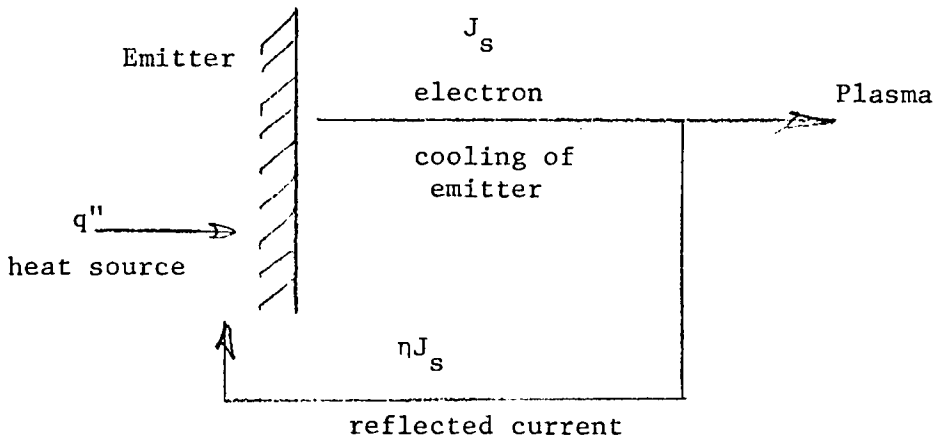


Fig. 19. Emitter Electron Cooling Changes

The increase in return current is equal to the decrease in output current from the diode. The change in energy returned to the emitter is equal to the output current multiplied by the product of the fractional increase in return current, the average energy of those electrons and the conversion efficiency. For small changes in  $q''$ , then from Eq. (4-2),

$$\Delta E_o = \beta J \left(1 - \frac{\Gamma}{\Gamma_o}\right) (2k T_{eE} + eV_E) \quad , \quad (4-3)$$

where

$\Delta E_o$   $\equiv$  change in output power (watts/cm<sup>2</sup>)

$\beta$   $\equiv$  efficiency

$\Gamma/\Gamma_o$   $\equiv$  output change due to plasma transport changes

$2kT_{eE}$   $\equiv$  average thermal energy of an electron at the emitter side of the plasma which escapes the plasma potential well (eV)

$eV_E$   $\equiv$  plasma potential sheath at the emitter side (eV).

The last term comes about by considering that electrons reflected from the plasma on the emitter side of the diode will gain the potential energy ( $eV_E$ ) plus the kinetic energy it possessed originally ( $2kT_{eE}$ ).

The energy returning to the emitter is going to raise the temperature of the emitter. The approximations made here therefore only apply for very low inert gas pressures.

The saturation current, electron temperature, and particle current ratios were determined earlier and the values for the emitter sheath were determined from Fig. 5.

It is assumed that the emitter sheath will not change in magnitude. The efficiency is found by summing all the energy transfer modes and dividing these into the cell output, the efficiency calculated in this way is 21.3%. Although this figure is high, the absence of conduction losses through leads, insulators, and other components would explain the diodes relatively good efficiency.

Figure 20 presents the results from Eq. (4-3), showing that, for a constant efficiency, the power output will rise slightly due to the

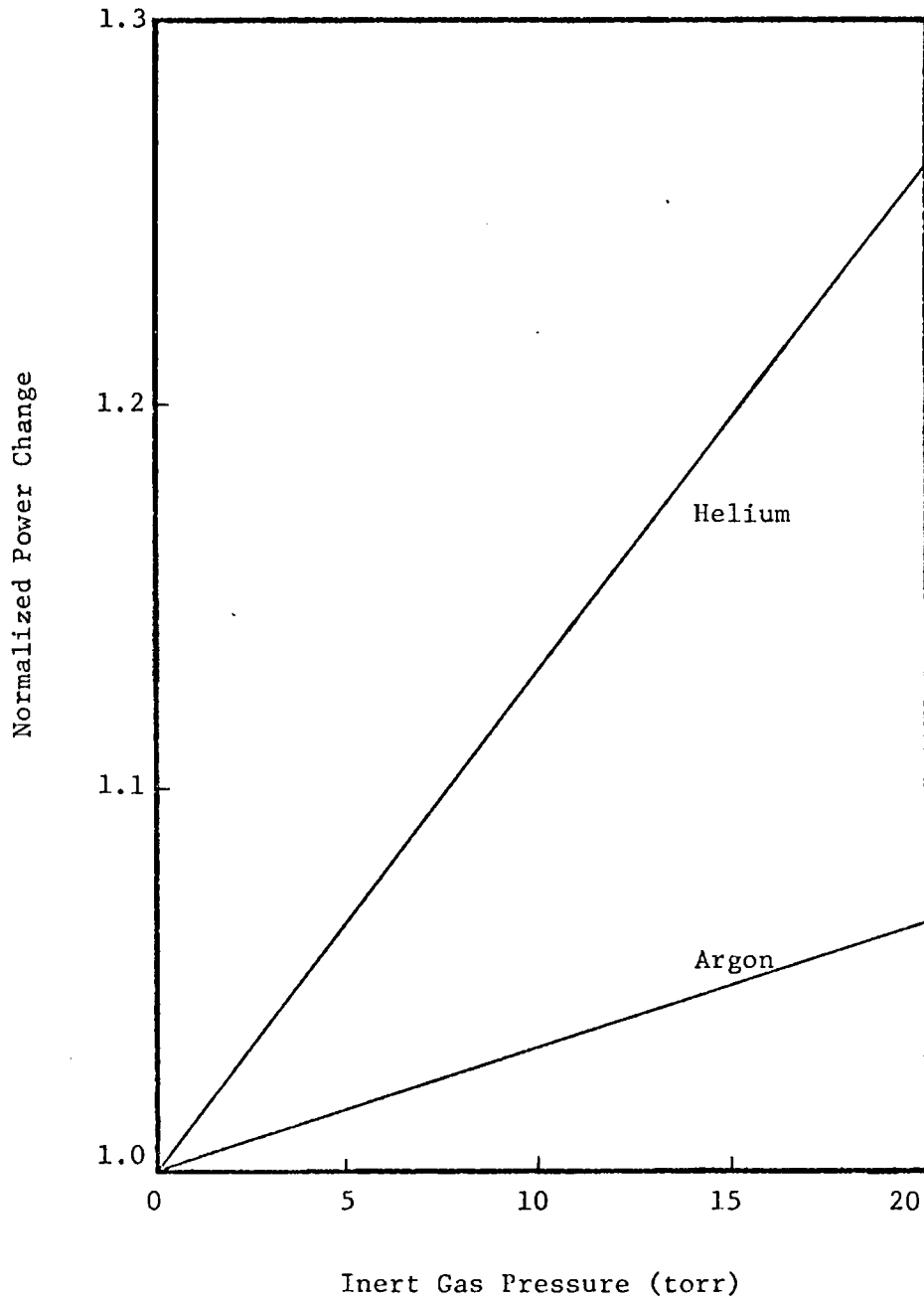


Fig. 20. The Change in Power Output with Gas Pressure Due to Current Reflection

added heat source of the plasma reflected electron current. This method of approach is an approximation to the energy balance method described in Appendix C.

### Inert Gas Energy Transfer

Inert gas heat conduction will vary with pressure, and have the effect of increasing the heat conduction losses across the cell, thereby reducing the amount of energy available for conversion.

The inert gas energy transport will be by conduction, and therefore will obey the equation:

$$q_I = \frac{T_E - T_c}{R_I} \quad (4-5)$$

where

$q_I \equiv$  net helium energy transport

$R_I \equiv$  inert gas conduction resistivity

$$= \frac{L}{Ak}$$

$L \equiv$  diode spacing (cm)

$A \equiv$  one square centimeter

$k \equiv$  thermal conductivity coefficient (watts/cm<sup>2</sup>-°K).

All of the constants required to calculate the heat transfer  $q_I$  are specified by the diode parameter except the thermal conductivity coefficient  $k$ .

The variation of the conductivities of helium and argon have been measured with respect to pressure.<sup>17</sup> The data presented is for a

specific spacing and is a composite of several sets of super-imposed data. Figure 21 presents the data from Prigogine and Waelbroeck.<sup>17</sup>

The authors state that the graph is the result of adjusting the data from three different size cells to overlap by adding a constant to the log of the pressure, thereby arriving at the adjusted pressure,  $p^*$ .

The conductivities of various sized cells can be calculated if it is realized that the ratio of mean-free-path to gap width is a constant for the "break-over" point of transition from the Knudsen regime to higher pressures. Thus, to determine the conductivities for the case being considered the  $\lambda/d$  ratios of the original data are calculated, and then the mean-free-path for a different gap width is calculated. This mean-free-path is then translated into equivalent pressure and this becomes the new "break-over" point. Figure 22 presents the conductivity data for the gap width of 2.08 mils.

For purposes of the calculation the general shape of the curve is assumed to be constant with increasing pressures, and the atmospheric pressure conductivities are taken at 1500°C to be  $4.94 \cdot 10^{-3}$  (watts/cm°K) for helium and  $0.738 \cdot 10^{-3}$  (watts/cm°K) for argon.<sup>17</sup>

Using Fig. 22 and Eq. (4-5) the net heat transfer is given in Fig. 23 for inert gas pressures of 0-20 torr in Fig. 23.

Energy losses out the gap sides on experimental diodes can become considerable, as shown in Appendix B.

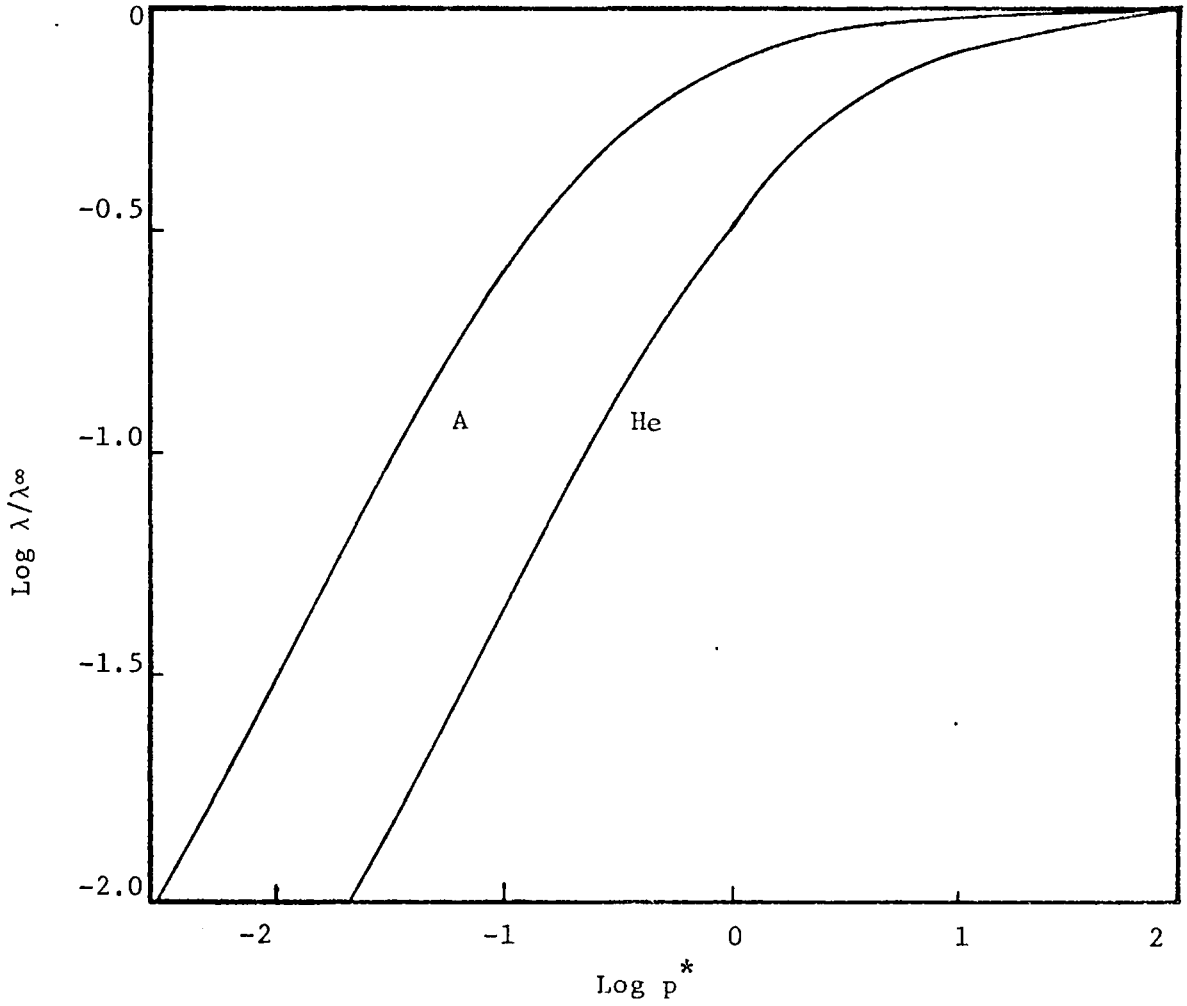


Fig. 21. Thermal Conductivities  $\lambda$  of Helium and Argon as a Function of Pressure.  $\lambda^\infty$  Observed Thermal Conductivity at Atmospheric Pressure.

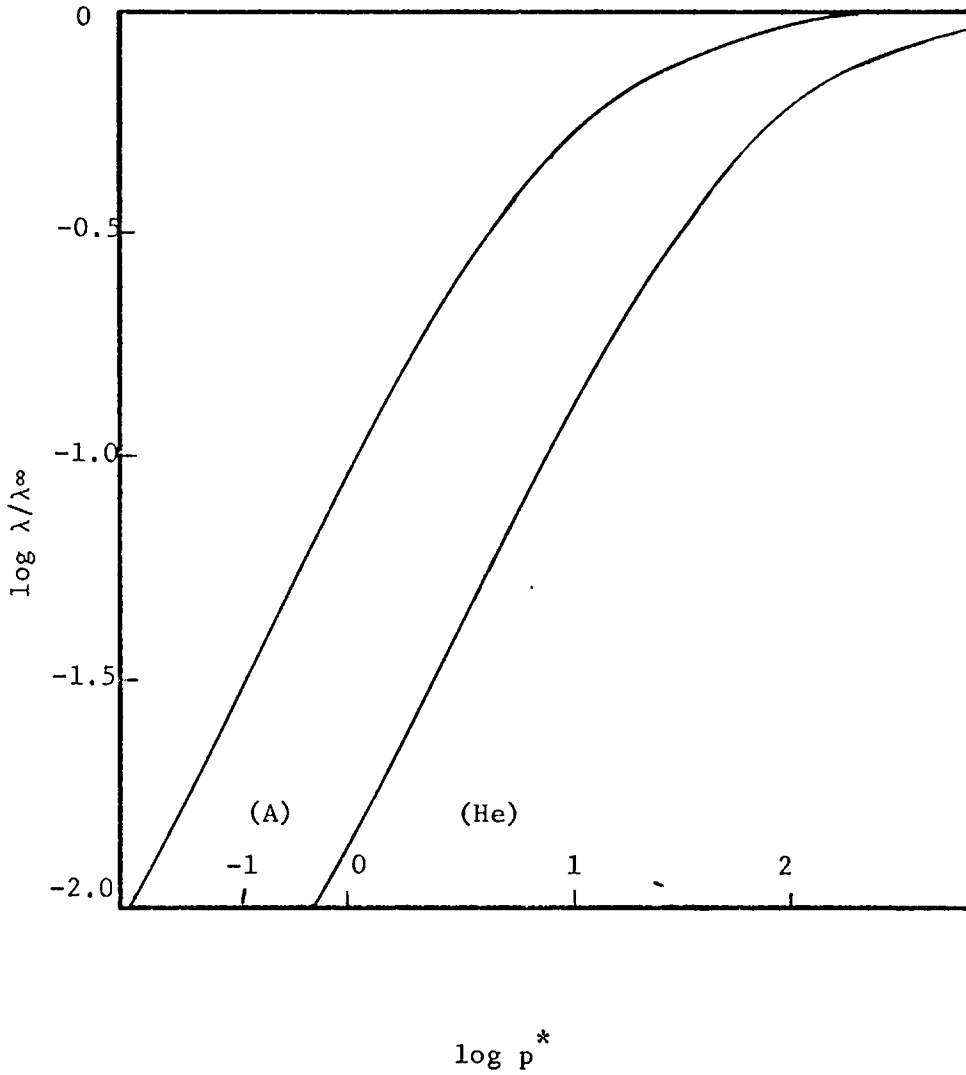


Fig. 22. Thermal Conductivities  $\lambda$  of Helium and Argon as a Function of Pressure for a 2 mil gap, where  $p^* \equiv 1$  torr and  $\lambda^\infty \equiv$  Conductivity at Atmospheric Pressure

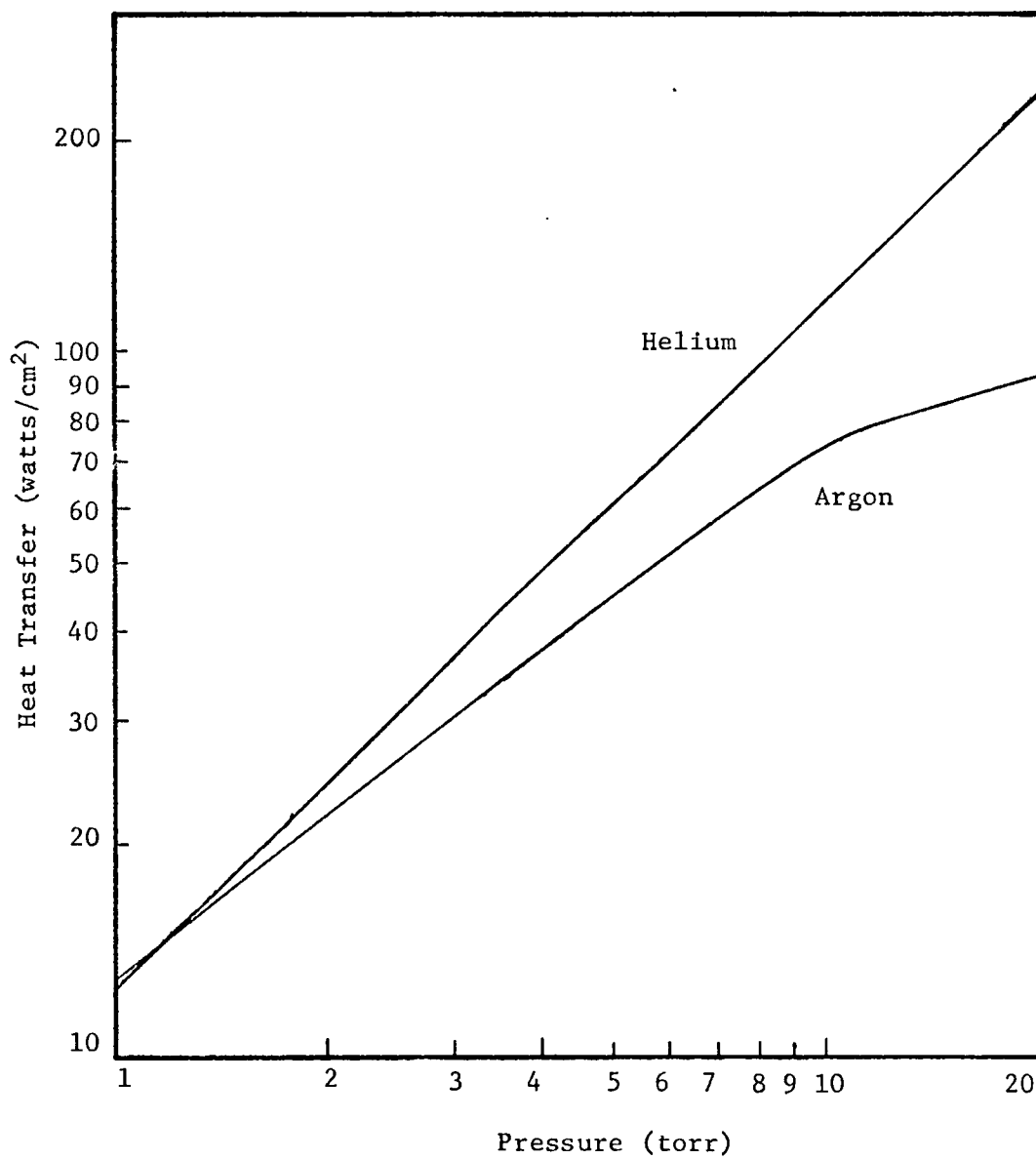


Fig. 23. Inert Gas Heat Transfer (watts/cm<sup>2</sup>) versus Inert Gas Pressure (torr) for a Gap of 2 mils and  $\Delta T = 1000^{\circ}\text{K}$

## CHAPTER 5

### CONCLUSIONS AND RESULTS

There are several points of interest which should be emphasized in analyzing the results.

Chapter 3 presents the effect of inert gas upon the diode output due to changes in the plasma properties. This mechanism of change is considered separately from the changes in heat transfer because the mechanisms, though they both effect the output of the diode, are completely separate in the way in which they effect the output.

The only overlap of these two, the plasma changes, and the energy transport changes occurs when one considers the changes in heat transfer due to electron kinetic energy transport. This term is reduced by the addition of helium, and thereby brings about an effective insulation of the emitter. This loss of electron cooling by the emitter might explain the increases Backus<sup>6</sup> saw in emitter temperature as inert gases were introduced.

The question of why the effective albedo of the plasma increases so much with increases in the inert gas pressure is a valid one if the cesium and inert gas cross-sections are compared. This author feels the albedo changes come about because of changes in the density of cesium ions in the plasma as a result of reduced volume ionization. It is postulated that the addition of the inert gases to the diode reduce the chances of a high energy electron ionizing a cesium atom. In addition

a rise in space-charge effects occurs from the formation of a charge layer of electrons near the emitter from inert gas scattering of those electrons. The effect is to drive a larger fraction of the electrons back into the emitter, thereby increasing the albedo.

The effects of the various mechanisms involved upon the diode output are summarized in Fig. 24.

It is noted that the heat conduction by inert gases is the dominating factor. The effect is dependent upon the emitter to collector distance, and doubling this distance would effectively halve these losses.

The effect of the inert gas here is approximated by assuming the available source power for the diode is divided among the various transfer mechanisms proportionately to the transfer coefficients. Thus the power would go to one half when the inert gas transfer was equal to all the other modes combined.

Figure 25 gives the resultant power losses for the model considered.

Figure 26 compares the results of this model with data presented in the literature,<sup>5,6</sup> with the appropriate changes in inert gas conduction. The temperatures were not changed to conform with the experimental values. The lower temperatures of the diode operation would reduce the effect of inert gas transfer somewhat.

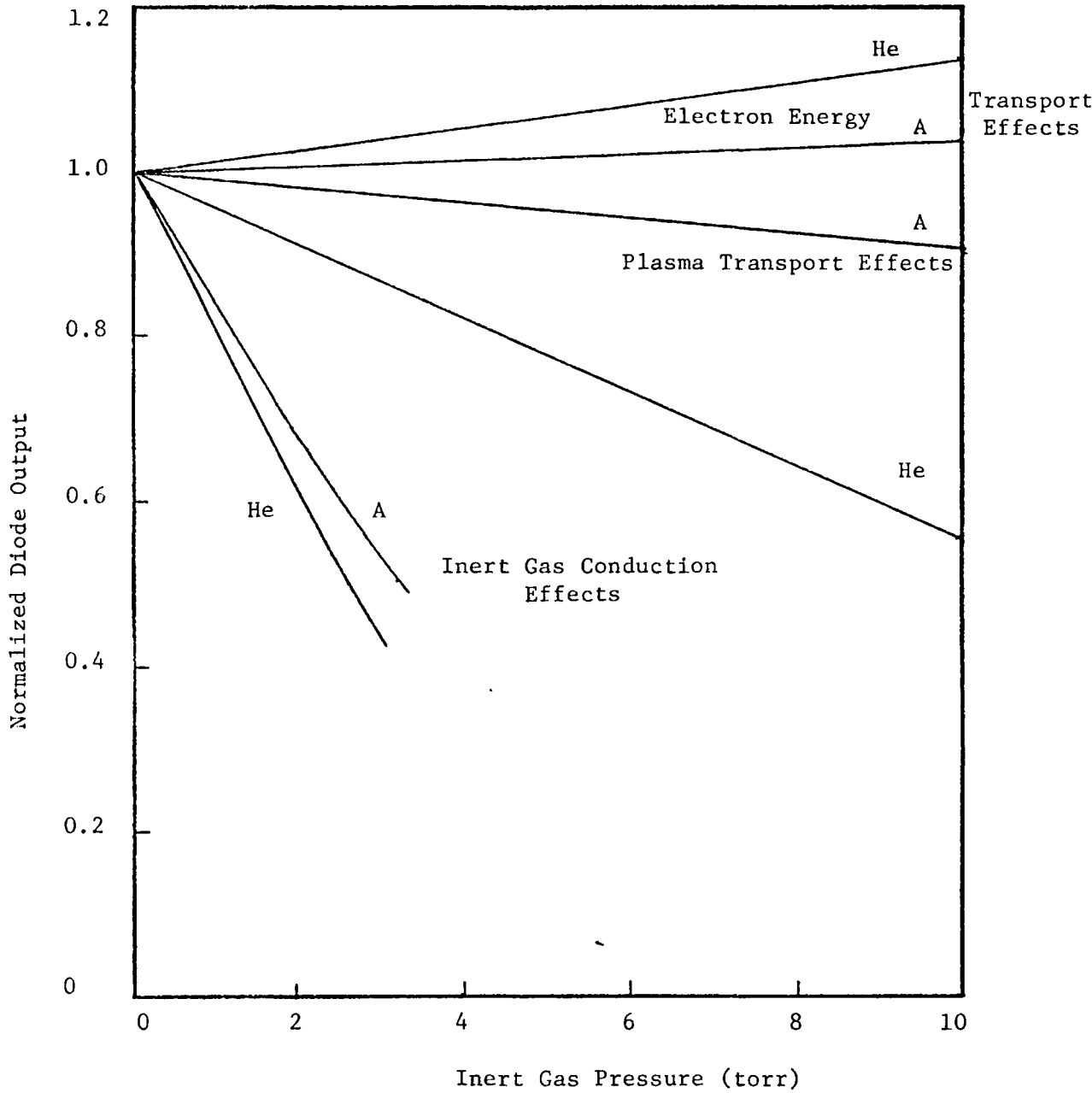


Fig. 24. Summary of the Effects of Inert Gas Introduction on a Cesium Thermionic Diode with a 2 mil Spacing and  $T_{cs} = 645^{\circ}\text{K}$

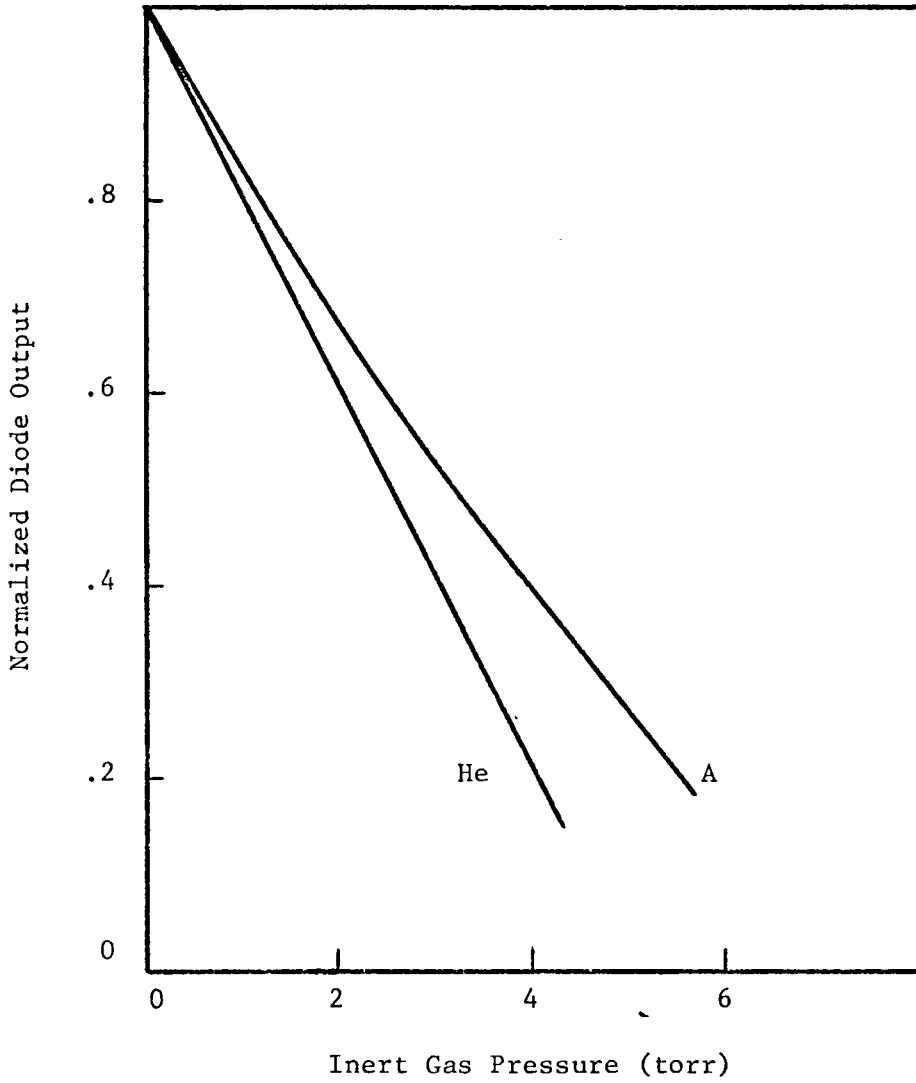


Fig. 25. Normalized Diode Output versus Inert Gas Overpressure for a 2 mil Spacing

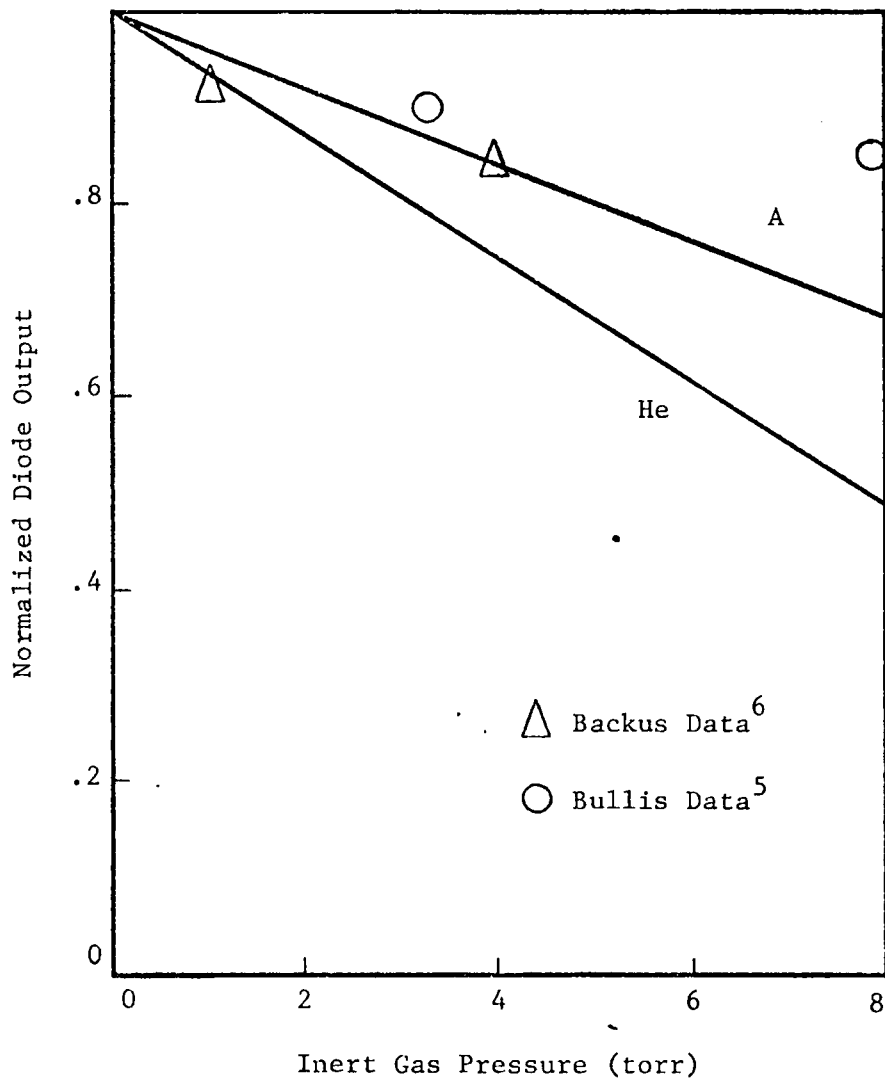


Fig. 26. Normalized Diode Output versus Inert Gas Overpressure for a 10 mil Spacing, with Experimental Data Plotted for Argon Only

## APPENDIX A

### DIFFUSION OF ELECTRONS THROUGH THE PLASMA<sup>10</sup>

Assume a neutral field free plasma bounded by emitter and collector, and with no significant source or sink of electrons within the plasma. The following is true:

$$\frac{d^2n}{dx^2} = 0 \quad (\text{A-1})$$

where  $n$  is the density of electrons. The solution is

$$n = Mx + N \quad (\text{A-2})$$

where  $M$  and  $N$  are constants determined by boundary conditions.

At the emitter side of the plasma the electron current entering the plasma ( $x=0$ ) is:

$$\frac{n_e \bar{v}}{4} + \frac{J}{2} = J_s + \left( \frac{n_e \bar{v}}{4} - \frac{J}{2} \right) (1 - \exp(-V_E/kT_{eE})) \quad (\text{A-3})$$

similarly at  $x=d$ , the collector side:

$$\frac{n_e \bar{v}}{4} - \frac{J}{2} = J_{es} + \left( \frac{n_e \bar{v}}{4} - \frac{J}{2} \right) (1 - \exp[-V_c/kT_{ec}]) \quad (\text{A-4})$$

where  $n_i$  and  $n_e$  are ion and electron number densities. Changes in the electron temperature are assumed to be nil.

Ficks law states that

$$J = \frac{\bar{v}\lambda}{3} \frac{dn}{dx} \quad . \quad (A-5)$$

Solution to the above equations have been accomplished, and the final equation is presented as:

$$J_s/J = a + b\left(\frac{d}{\lambda}\right) \quad (A-6)$$

where

$$a = \frac{\exp(V_E/kT_{cE}) + \exp(V_c/kT_{ec}) - 1}{\exp(V_E/kT_{eE}) - \frac{J_{cs}}{J_s} \exp(V_c/kT_{ec})} \quad ,$$

and

$$b = \frac{3/4}{\exp(V_E/kT_{eE}) - \frac{J_{cs}}{J_s} \exp(V_c/kT_{ec})}$$

and  $J_s$  and  $J_{cs}$  are the saturation emission currents from the emitter and collector respectively.

Assuming the collector emission is negligible Eq. (2-9) may be produced.

## APPENDIX B

### ENERGY TRANSPORT FROM THE INTERELECTRODE SPACE

The energy transport out of the gap can be a significant effect in the energy flow from the emitter to collector.

To find the net energy transport due to differences in the temperature of the gas between the electrodes and the gas outside this volume, consider an imaginary window between the two volumes. Because there is no pressure difference there is no net gas flow, and therefore the equality of pressures on side 1 with side 2 gives:

$$n_1 m_1 v_1 = n_2 m_2 v_2 \quad (\text{B-1})$$

where  $n_1$  is the number of atoms/cm-sec of side 1 striking the imaginary window,  $m_1$  is the mass of those atoms, g and  $v_1$  is their velocity (cm/sec). Similarly  $n_2$ ,  $m_2$ , and  $v_2$  apply to side 2. Assuming monatomic gases, then the velocity is given by:

$$v_1 = \sqrt{\frac{3kT_1}{m_1}} \quad (\text{B-2})$$

and similarly  $v_2$ .

Modifying Eq. (B-1) gives

$$n_2 = n_1 \frac{v_1}{v_2} \quad (\text{B-3})$$

Substituting Eq. (B-2) into Eq. (B-3) gives:

$$n_2 = n_1 \sqrt{T_1/T_2} . \quad (\text{B-4})$$

This will give the ratio of density of the gas atoms on either side striking the window.

The net energy transferred by gas atoms passing through the window plane is given by:

$$E_N = KE_1 - KE_2$$

where  $KE_1$  is the energy transported by  $n_1$  molecules passing through the imaginary surface and similarly  $KE_2$  the energy transported through the window by  $n_2$ . Thus:

$$E_N = \frac{1}{2} n_1 m_1 v_1^2 - \frac{1}{2} n_2 m_2 v_2^2 . \quad (\text{B-5})$$

Assuming again monatomic atoms carrying  $3/2kT$ , then Eq. (B-5) becomes:

$$E_N = 3/2 n_1 k T_1 - 3/2 n_2 k T_2 . \quad (\text{B-6})$$

Recalling Eq. (B-4), thus:

$$E_N = 3/2 k n_2 (\sqrt{T_1 T_2} - T_2) . \quad (\text{B-7})$$

Thus, if  $T_1$  is considered to be the average of the emitter and collector temperatures (1500°K) and  $T_2$  the reservoir temperature (645°K) then the power loss due to transport out the gap between the electrodes is presented in Fig. B-1.

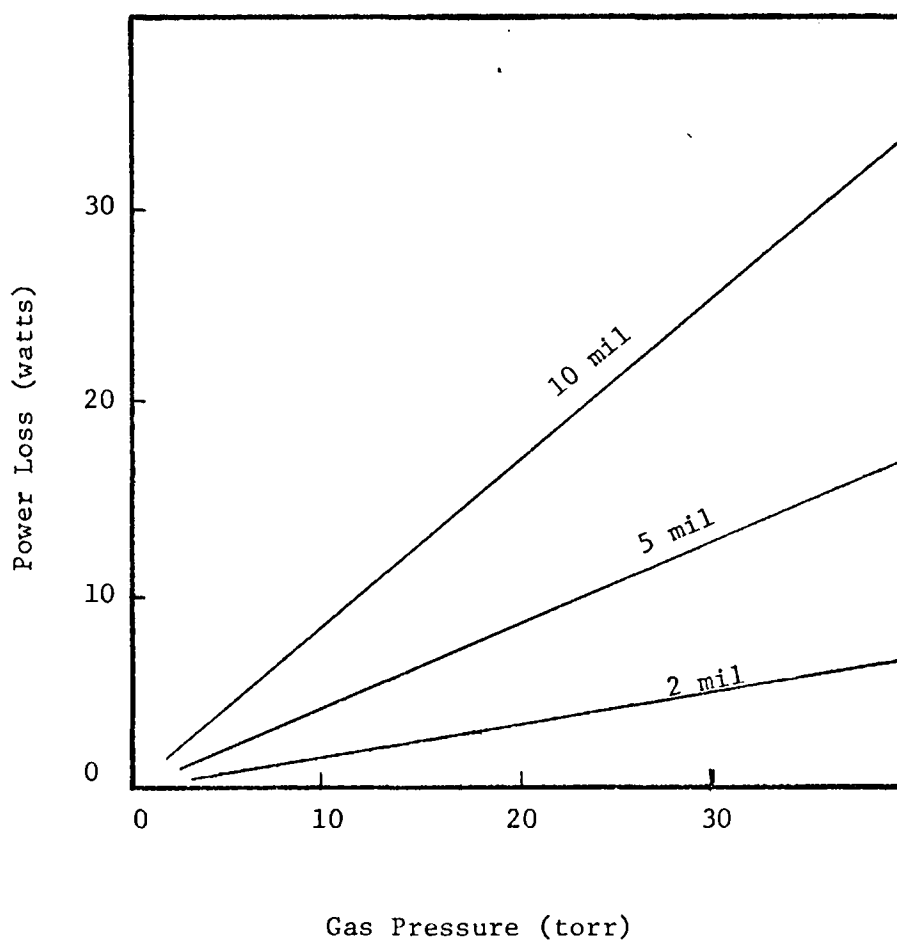


Fig. B-1. Power Loss from Interelectrode Gap Due to Gas Transport at Various Spacings, Assuming a One Inch Diameter Planar Electrode Diode

## APPENDIX C

### ENERGY BALANCE ON THE EMITTER

Assume an emitter surface whose temperature is governed by the following mechanisms:

- 1)  $q_s$   $\equiv$  heat source
- 2)  $q_{cs}$   $\equiv$  cesium conduction
- 3)  $q_R$   $\equiv$  radiant transfer
- 4)  $q_I$   $\equiv$  inert gas transport
- 5)  $q_{ec}$   $\equiv$  electron cooling
- 6)  $q_{en}$   $\equiv$  electron heating

All of the above are expressed in watts/cm<sup>2</sup>

An energy balance requires:

$$q_s + q_{en} = q_{cs} + q_R + q_I + q_{ec} \quad (C-1)$$

The individual terms are given by:

$$q_s = \text{constant (temperature independent)}$$

$$q_{cs} = K_{cs} (T_E - T_c)$$

$$q_R = K_{R1} T_E^4 - K_{R2} T_c^4$$

$$q_I = K_I (T_E - T_c)$$

$$q_{ec} = J_s (2kT_E)$$

$$q_{eh} = (J_s - J) (2kT_{eE} + V_E)$$

where

$K_{cs} \equiv$  cesium conductivity coefficient

$$= \frac{k_{es}}{L} \quad (\text{watts/cm}^2\text{-}^\circ\text{K})$$

$K_{R1} =$  emitter radiation transfer coefficient

$$= \frac{\sigma}{\frac{1}{\epsilon_E(T_E)} + \frac{1}{\epsilon_c(\sqrt{T_E T_c})} - 1}$$

$$= (\text{watts/cm}^2\text{-}^\circ\text{K}^4)$$

$K_{R2} =$  collector conductivity coefficient

$$= \frac{\sigma}{\frac{1}{\epsilon_E(\sqrt{T_E T_c})} + \frac{1}{\epsilon_c(T_c)} - 1}$$

$$= (\text{watts/cm}^2\text{-}^\circ\text{K}^4)$$

$K_I =$  inert gas conductivity coefficient

$$= \frac{k_I}{L} \quad (\text{watts/cm}^2\text{-}^\circ\text{K}).$$

At this point the definition of an albedo  $\eta$  is made such that:

$$J_s - J = \eta J_s$$

or

$$\eta = 1 - \frac{J}{J_s} \tag{C-2}$$

Using Eq. (C-2), and the equations stated for the heat fluxes:

$$\begin{aligned}
& q_s + \eta J_s (2kT_{eE} + eV_E) \\
& = K_{cs} (T_E - T_c) + K_R (T_E^4 - T_c^4) + K_I (T_E - T_c) \\
& + J_s (2kT_E) .
\end{aligned} \tag{C-3}$$

Realizing

$$J_s = AT_E^2 e^{-\phi_E/kT_E}$$

then:

$$\begin{aligned}
& q_s + \eta AT_E^2 e^{-\phi_E/kT_E} (2kT_{eE} + eV_E) \\
& = K_{cs} (T_E - T_c) + K_R (T_E^4 - T_c^4) + K_I (T_E - T_c) \\
& + AT_E^2 e^{-\phi_E/kT_E} (2kT_E) .
\end{aligned} \tag{C-4}$$

An assumption which simplifies the above is to assume the temperature of the electrons at the emitter side of the plasma is given by:

$$3/2 kT_{eE} = eV_E + 2kT_E$$

or

$$T_{eE} = \frac{2eV_E}{3k} + \frac{4}{3} T_E . \tag{C-5}$$

Incorporating Eqs. (C-5) and (C-6) gives:

$$\begin{aligned}
& q_s + \eta AT_E^2 e^{-\phi_E/kT_E} (7/3 eV_E + 8/3 kT_E) \\
& = K_{cs} (T_E - T_c) + K_R (T_E^4 - T_c^4) + K_I (T_E - T_c) \\
& + 2Ak T_E^3 e^{-\phi_E/kT_E} .
\end{aligned} \tag{C-6}$$

| Then

$$\begin{aligned}
 & K_{R1} T_E^4 - (8/3 k \eta A - 2 k A) T_E^3 e^{-\phi_E/kT_E} \\
 & - 7/3 \eta A e V_E T_E^2 e^{-\phi_E/kT_E} + T_E (K_{CS} + K_I) \\
 & - q_s - T_c (K_{CS} = K_I) - K_{R2} T_c^4 = 0 . \qquad (C-7)
 \end{aligned}$$

By assuming the emitter sheath does not change substantially with inert gas pressure, and similarly that the emissivities do not change Eq. (C-7) can be solved for changes in the emitter temperature due to changes in the inert gas pressure.

It should be noted that if the albedo rises much more quickly than the conduction due to inert gas then the temperature of the emitter will rise to compensate. This is possibly an explanation for the temperature rises seen by Backus.<sup>6</sup> Also it is noted that removing the load from a diode will increase the emitter temperature to accommodate for lost electron cooling.

#### REFERENCES

1. Coombe, R. A., An Introduction to Direct Energy Conversion; Sir Isaac Pitman and Sons Lmtd., London, 1968, pp. 54-83.
2. Kettani, M. A., Direct Energy Conversion, Addison-Wesley Publishing Co., Reading, Massachusetts, 1970, pp. 182-211.
3. Blue, E., and Ingold, J. H., Direct Energy Conversion, edited by G. W. Sutton, McGraw-Hill Book Company, San Francisco, California, 1966, pp. 239-259.
4. Kaplan, C., and Merzenich, J. B., "Xenon Addition Experiment in a Thermionic Converter", Proceedings of Thermionic Conversion Specialists Conference, Cleveland, Ohio, October 26-28, 1964, p. 333.
5. Bullis, R. H., Wiegand, W. J., and Bell, D. W., "Effects of Inert Gas Overpressure on Arc Characteristics," Proceedings of Twenty-Fifth Annual Conference on Physical Electronics, Cambridge, Massachusetts, March 24-26, 1965, p. 11.
6. Backus, Charles Edward, "The Effect of Impurity Gas on the Operation of a Thermionic Cesium Diode," Ph.D. Dissertation, University of Arizona, 1966.
7. Razor, N. S., "Practical Aspects of Fundamental Research in Thermionic Conversion," Office of Naval Research Final Technical Report, Contract N00014-69-C-0279, Sept., 1, 1969.
8. Reichelt, W. H., "Electron Temperature and Ion Density in a Cesium Plasma Diode," Proceedings of the Thermionic Conversion Specialists Conference, Cleveland, Ohio, Oct., 26-28, 1964.
9. Talaat, M. E., "The Surface Ionization and Volume Ionization Modes of Operation in the Thermionic Plasma Energy Converter," Advanced Energy Conversion, Vol. 2, pp. 447-458, Pergamon Press, 1962.
10. Razor, N. S., "Analytical Description of Cesium Diode Phenomenology," International Conference on Thermionic Electric Power Generation, London, 1965.
11. Delacroix, Jean L., Introduction to the Theory of Ionized Gases, Interscience Publishers, Inc., New York, 1960.

12. Rose, David J., and Clark, Melville, Plasmas and Controlled Fusion, M.I.T. Press and John Wiley and Sons Inc., New York, 1961.
13. Flavin, R. K., and Meyerand, R. G., Jr., "Collision Probability of Low Energy Electrons with Cesium Atoms," Advanced Energy Conversion, Vol. 3, pp. 3-18, Pergamon Press, 1963.
14. Houston, John M., "Cross Section Values to Use in Analyzing the Cesium Thermionic Converter," Thermionic Conversion Specialists Conference, Cleveland, Ohio, Oct. 26-28, 1964.
15. Thermionic Research Computation Aids, by Thermo Electron Corp., Waltham, Massachusetts, January 1968.
16. McCandless, R. J., and Hill, P. R., Radiation Heat Transfer Calculations, Thermionic Conversion Specialists Conference Palo Alto, California, Oct. 30-Nov. 1, 1967, pp. 370-375.
17. Prigogine, I., and Waelbroeck, F., "Heat Conductivity and Chemical Reactions in Gases," Proceedings of the Joint Conference on Thermodynamic and Transport Properties of Fluids. London, July 10-12, 1957, pp. 128-132.
18. Handbook of Chemistry and Physics, 50th Edition, The Chemical Rubber Company, Cleveland, Ohio, 1970, p. E-1.

